Uncovering the Depths of the Human Proteome: Antibody-based Technologies for Ultrasensitive Multiplexed Protein Detection and Quantification

Authors
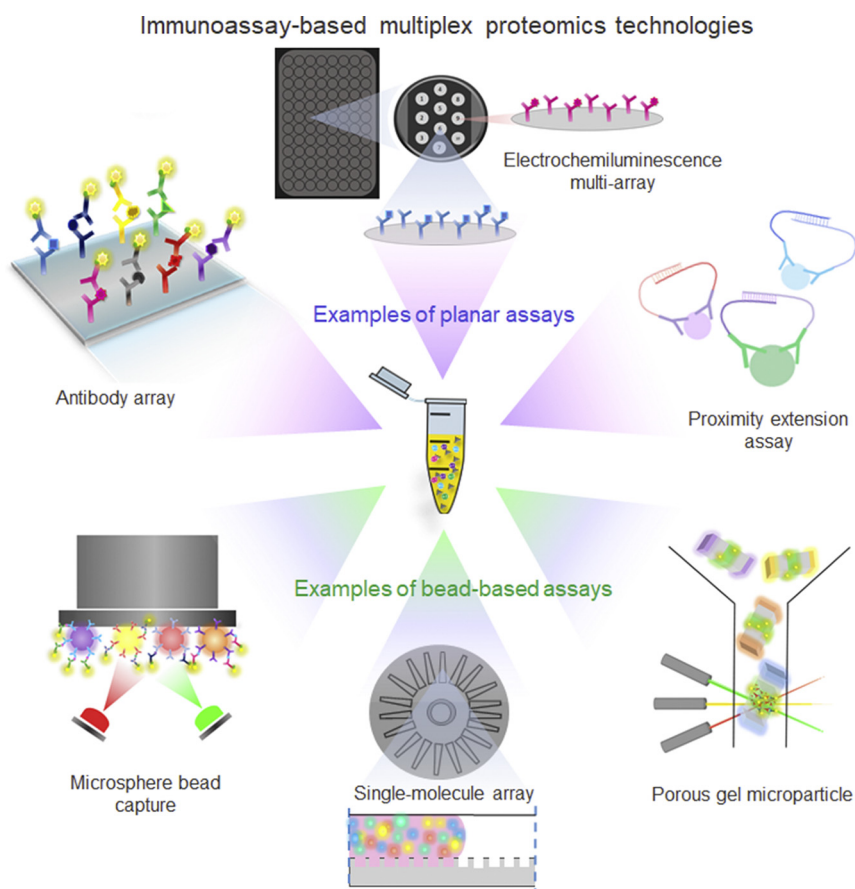Annie H. Ren, Eleftherios P. Diamandis, and Vathany Kulasingam

Correspondence
vathany.kulasingam@uhn.ca

In Brief
Probing the human plasma proteome is attractive for biomarker and drug target discovery. Recent breakthroughs in multiplex proteomics technologies enable the simultaneous and sensitive quantification of thousands of proteins in biofluids. We provide a comprehensive guide to the methodologies, performance, advantages, and disadvantages of established and emerging technologies for the multiplexed ultrasensitive measurement of proteins. Gaining knowledge on these innovations is crucial for choosing the right multiplexed proteomics tool to critically complement traditional proteomics methods.

Graphical Abstract

Highlights

- Immunoassay-based multiplex proteomics methods measure 1000+ proteins in biofluids.
- Multiplex protein measurements alleviate demands on time, cost, and sample volume.
- This guide helps researchers choose the most suitable tool for their applications.

Uncovering the Depths of the Human Proteome: Antibody-based Technologies for Ultrasensitive Multiplexed Protein Detection and Quantification

Annie H. Ren[1,2]**, Eleftherios P. Diamandis**[1,2,3]**, and Vathany Kulasingam**[1,3,*] (iD)

Probing the human proteome in tissues and biofluids such as plasma is attractive for biomarker and drug target discovery. Recent breakthroughs in multiplex, antibody-based, proteomics technologies now enable the simultaneous quantification of thousands of proteins at as low as sub fg/ml concentrations with remarkable dynamic ranges of up to 10-log. We herein provide a comprehensive guide to the methodologies, performance, technical comparisons, advantages, and disadvantages of established and emerging technologies for the multiplexed ultrasensitive measurement of proteins. Gaining holistic knowledge on these innovations is crucial for choosing the right multiplexed proteomics tool for applications at hand to critically complement traditional proteomics methods. This can bring researchers closer than ever before to elucidating the intricate inner workings and cross talk that spans multitude of proteins in disease mechanisms.

Studying the proteome is central to understanding the functional units of a cell. Proteins are involved in a breadth of biological processes, from apoptosis, to cellular checkpoints, to inflammation to name a few, all of which are pertinent to diseases ranging from cancer, to neurodegenerative, cardiovascular, and infectious diseases (1–3). Studying the alterations in protein expression, secretion, and interactions in biological fluids can elucidate disease pathways and discover novel therapeutic targets and noninvasive biomarkers (4, 5). Recent breakthroughs in immunoassay-based multiplex protein technologies now allow for the simultaneous quantification of hundreds to thousands of proteins in a single assay. However, applying these novel platforms to map the circulating disease proteome requires superb technical sensitivity to detect scarce disease-associated proteins, excellent reproducibility, and cost-effective means for robustly powered validation studies and clinical trials in the arduous effort of bringing a novel drug or biomarker to the clinic. When it comes to clinical practice, the technical demands further increase with added expectations of realistic sample volume requirement and turnaround time. Equipped with a growing array of ultrasensitive multiplex proteomics technologies, selecting the right tool for the question at hand can be daunting without first acquiring considerable knowledge surrounding the variety of technologies. We herein provide a comprehensive guide of the technological principles, performance, strengths, and weaknesses of commercial immunoassay-based technologies for the multiplexed ultrasensitive measurement of proteins in human biofluids. The principles, advantages, and drawbacks of some of the technologies described in this Review have been reviewed elsewhere (6–9). In these cases, we provide updates on the rapidly evolving field, where advancements in the multiplexing capability and analytical prowess of the technologies are unveiled on a yearly basis, to enable researchers to discover more of the human proteome.

CHALLENGES IN PROTEIN DETECTION AND MEASUREMENT

Unlike the rapid advances in whole genome sequencing, traditional proteomics methods have lagged behind in terms of improving throughput and sensitivity for measuring proteins in biofluids at the proteome-wide scale. In comparison with the genome, which consists of about 20,000 genes, the proteome is far more complex with an estimated close to one million proteins, after accounting for alternative splicing and posttranslational modifications (1). It is therefore unsurprising that it takes decades to develop the incredibly powerful technical methods required to chart the complete human proteome, let alone unravel how protein expression dynamically changes in various diseases (10).

Mass spectrometry (MS) remains the core tool for proteomics efforts, with the two main methodologies for the wide detection of proteins being bottom-up and top-down MS (reviewed elsewhere) (11–13). Bottom-up MS is 100-fold more

sensitive than the latter method and is favored for discovery-based proteomics for its broader coverage and higher throughput (11). Though capable of detecting up to several thousand proteins in a single liquid chromatography (LC)-MS/MS experiment, the method may hold bias toward high-abundance proteins and delivers less robust detection of low-abundance proteins (13). When it comes to using complex biological matrices such as human serum or plasma, the performance of MS techniques further deteriorates with even targeted methods typically unable to detect proteins below low μg/ml or high ng/ml levels without extensive sample fractionation or enrichment to decrease the sample complexity (14). To this end, the utility of MS for identifying novel cancer biomarkers or drug targets is hindered by insufficient resolution of the human proteome (15). The typical dynamic range of LC MS/MS is 4- to 6-log, while proteins in biofluids can span 12-log in concentration (13). Paired with limited sensitivity, MS methods may often fall short on detecting clinically relevant proteins, where candidate biomarkers with clinical applicability are often present in the sub pg/ml to sub ng/ml range (14). For example, aberrant protein structure and expression have been implicated in many cancers and neurodegenerative diseases (5, 16, 17). However, clinically relevant proteins in these diseases, such as brain-enriched proteins, tumor-related proteins, and cytokines, are secreted into extracellular fluids or leaked into the circulation at extremely minute concentrations (sub pg/ml or lower), thereby being virtually undetectable *via* MS methods without various fractionation and enrichment (13, 15). The numerous configurations and advancements in targeted MS-based techniques, such as selective reaction monitoring and parallel reaction monitoring, for multiplexed protein measurement are beyond the scope of this review and have been reviewed elsewhere (18–20). However, it is notable that progress in targeted MS techniques for quantifying proteins in biological matrices has gradually reached detection limits as low as 50 to 100 pg/ml (14, 21). However, the techniques may see hampered multiplexing capability to about 20 to 30 analytes being measured in a single assay (14, 21).

Tackling the drawbacks of MS-based approaches, a new generation of multiplexed proteomics technologies has steadily gained traction with the goal of heightening sensitivity while augmenting multiplexing abilities. The technologies came from innovations on the enzyme-linked immunosorbent assay (ELISA), which is the most used tool for protein quantification in research settings and the gold standard of clinical laboratories for detecting single analytes. ELISAs achieve 1 to 10 pg/ml detection limits with no need for sample pretreatment (22). The sandwich ELISA takes advantage of a pair of antibodies that recognize different epitopes on a target antigen to enable the detection of proteins in complex biofluids with high specificity. However, measuring multiple analytes by performing numerous ELISA immunoassays becomes tedious and impractical owing to substantial demands on sample volume requirement, (which can be as high as 50 μl of sample per analyte), turnaround time, and cost.

Multiplex measurements offer the unique opportunity to gain a holistic view of the biochemically complex environments involved in pathogenesis and responses to treatment, with alleviated demands on time, cost, and sample volume. From a practicality standpoint, human biological samples from clinical settings are often restricted in availability and quantity. Therefore, multiplexing appeals to researchers for comprehending intricate physiological conditions with the convenience of a single, low-volume sample. The simultaneous detection of multiple protein analytes can come with sizeable obstacles, including nonspecific binding, interference, and cross-reactivity due to the different subpopulations of antibodies and intervening factors in complex matrices (23). Novel multiplexed proteomics technologies have created unique solutions to overcome these age-old challenges with fundamental differences in the assay format, where the reactions take place either on planar devices or microscopic beads. In the ensuing sections, we explain in detail some of the emerging and established commercial multiplex proteomics platforms currently available to equip researchers with a complete understanding of their advantages and limitations.

PLANAR IMMUNOASSAYS
Antibody Arrays

Antibody arrays are high-throughput forms of the traditional ELISA, where a large collection of distinct capture antibodies is immobilized onto a solid support surface (Fig. 1). The captured antibodies can be adapted to proteins of interest for the parallel analysis of multiple protein targets in a single sample. Commonly available antibody arrays are based on a sandwich or direct label format (Fig. 1), where their typical workflow and applications in basic and clinical research have been reviewed elsewhere (24). In general, sandwich formats may benefit from higher specificity as a pair of antibodies that recognize different epitopes of the antigen is used, and an assay signal is only generated when both antibodies have bound to the target. However, multiplexing may be compromised because all pairs of antibodies must be validated to avoid cross-reactivity rendering a practical capability of measuring between 10 and 80 analytes in each subarray (8). Multiple subarrays can be run in parallel to increase multi-analyte detection, although this increases the sample volume requirement.

The type of solid support used is also important for technical performance, with surfaces commonly made of glass or nitrocellulose membrane. Assays that utilize membrane-based supports generally rely on signal generation by fluorescence or chemiluminescence and are semiquantitative with an approximate 4-log dynamic range, where fold-change in protein concentration can be discerned by comparing signal intensity (8). These devices benefit from the convenience of
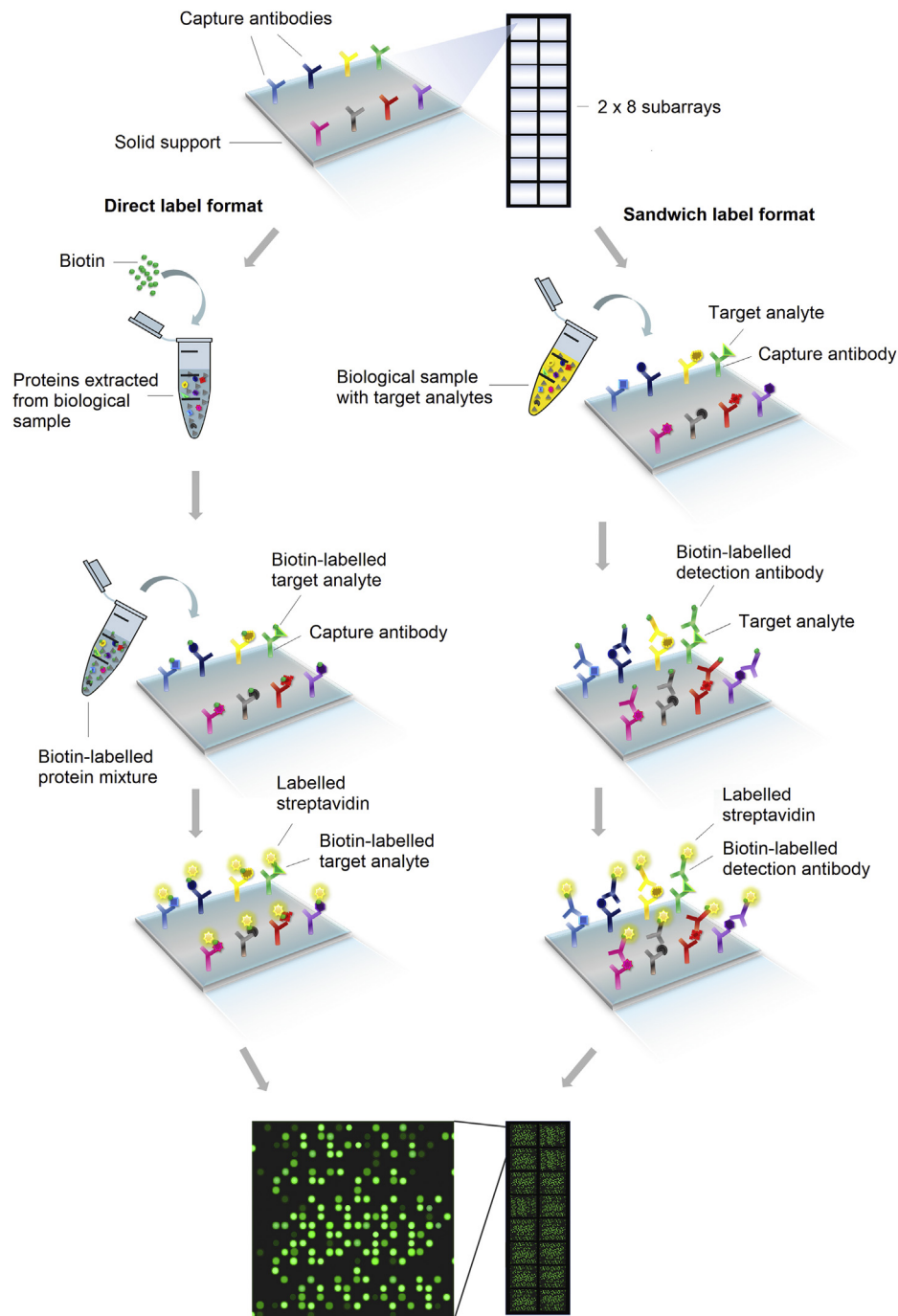
FIG. 1. **Antibody array.** Distinct capture antibodies are immobilized onto a solid support surface. Glass slide arrays are typically organized into 2 × 8 subarrays. In the direct label assay format, proteins from the biological sample are extracted and labeled with biotin. The processed sample is then incubated on the array to enable target analyte binding to the capture antibodies. After washing, labeled streptavidin is added, which binds to the biotin tags. The resulting signal is visualized by an array scanner. In the sandwich label format, the biological sample is directly incubated on the array to allow for target binding. After washing, the detection antibody, which is conjugated to a biotin tag, is added to form immunocomplexes. After more washing, labeled streptavidin is added to generate signal, as visualized by an array scanner.

easy processing akin to western blot membranes without the need of specialized equipment (8). Newer antibody arrays mostly use glass slides for solid support, as it allows for denser antibody printing, higher throughput, and multiplexing, while providing absolute protein quantification in some cases (8). Specialized for convenience and automation, glass slide

arrays that are spotted with distinct antibodies are typically organized into 2 × 8 subarrays, which emulate two columns of a 96-well microtiter plate, to allow for 16 samples to be analyzed on each slide (Fig. 1). The inclusion of protein standards in some technologies establishes a calibration curve of each analyte, thus permitting absolute quantification. Four slides can be arranged into a frame of the size of a 96-well plate to facilitate automation of the incubation and wash steps, which is critical for enhancing technical reproducibility. To further augment measurement reliability, the same capture antibodies are often spotted in several replicates on each subarray such that signal intensities are obtained as a mean of the readout from the technical replicates (8). Fluorescence intensity is the most common source for signal readout, where a microarray scanner is necessary for data acquisition. Advancements in glass-slide antibody arrays have proceeded at astonishing speeds where many technologies have improved in multianalyte detection by hundreds to thousands of proteins in the past 2 years. We provide an up-to-date list of commercial antibody array platforms and compare their technical performance (Table 1). In the following subsections, we examine three distinct antibody array technologies that offer some of the largest multiplexed protein libraries, to better understand their advantages and caveats for wide-scale proteomics screens.

Direct Label Array—The direct label antibody array offered by Full Moon Biosystems provides semiquantitative measurement of 60 to 1358 human proteins in parallel, with biological relevance in inflammation, cancer, cell cycle, and signaling pathways (25–29). Direct label antibody arrays benefit from higher multiplexing capability with hundreds to thousands of antibodies covalently immobilized on a glass-slide surface coated with 3-D polymer materials that enhance binding efficiency and specificity. Each antibody type is printed in 2 to 6 replicates to enhance data reliability. Workflow of the assay starts with protein extraction and labeling with biotin. The processed sample is then incubated on the array to enable the binding of analytes to the capture antibodies. Signal detection is facilitated by the addition of Cy3-labeled streptavidin to form fluorescent immunocomplexes that can be visualized by an array scanner. Signal intensity is extracted from the array images and normalized within each slide to determine fold changes in protein expression between samples. For each analyte, an average of the signal intensities from the technical replicates is determined, along with the coefficient of variation (CV), to address intraassay variation (30).

The main drawback to the direct label antibody arrays is the lack of absolute quantification of protein concentration. Due to this limitation, the dynamic range and sensitivity of the arrays are not well-established. Under optimized conditions, the assays can detect proteins in the ng/ml range in biological samples. However, as reported by the manufacturer, the CV between signal intensities from technical replicates can vary between 15% and 50% due to variations in sample preparation and array processing. Nevertheless, the arrays are advantageous for their low sample volume requirement, where 20 μl of serum/plasma is needed for analyzing up to 1358 proteins on a single slide. Each kit comes with two slides for processing two unique samples and costs approximately US$350 to $1580 depending on the array of analytes.

Competitive Protein Profiling—The competitive protein profiling arrays offered by Sciomics is used for direct comparisons of protein expression levels between two samples. The workflow relies on labeling the proteins extracted and purified from the two samples up for comparison with two different fluorescent dyes each, such that each sample has a distinct set of two fluorescent tags. The two samples are then mixed and incubated on typical glass-slide arrays, allowing for competitive binding of the target proteins to the large assortment of immobilized capture antibodies. Competition for the binding sites means the sample with a higher concentration of target proteins will bind more efficiently and prevalently to the capture antibodies, thus providing a direct comparison of protein concentration in the two samples. The array includes four technical replicates for each analyte. The array incubation and handling steps are fully automated to minimize variation. The final slide is scanned and processed through a four-channel excitation system to pinpoint the amount of each specific analyte from each of the two samples.

The comparative proteomics technology allows for the detection of 1300 human proteins in parallel in 10 μl of serum/plasma. The 1300 analytes of interest represent signaling pathway proteins, transcription factors, chemokines, and cytokines, as well as markers of apoptosis, cell stress, and oxidative stress (31–36). Quality control data by the manufacturer showed intra-assay variation of less than 10% CV for all analytes and sensitivity that is comparable or better than conventional ELISA, at sub ng/ml concentrations.

Micro-ELISA Array—The micro-ELISA array technology from RayBiotech combines 25 nonoverlapping glass-slide arrays to perform up to 1000 miniature sandwich ELISAs simultaneously, targeting mostly inflammation-related proteins, including cytokines, chemokines, growth factors, tumor markers, and transcription factors (37–43). Each 75 mm × 25 mm glass slide contains 16 identical antibody subarrays, where each subarray multiplexes 40 different proteins arranged in technical quadruplicates. The high-throughput array makes protein quantification 80 times more efficient than traditional ELISA, giving results in 4 h. Akin to a sandwich ELISA, capture antibodies are spotted onto each subarray. After sample incubation and washing, a biotinylated detection antibody is added. A streptavidin conjugated Cy3 dye is then conveyed, and the final resulting fluorescence signals are read *via* a microarray laser scanner. An absolute quantification of each analyte is calculated through the average of the technical quadruplicate values, after accounting for intra- and interslide normalization.

TABLE 1
Technical parameters of commercial antibody array platforms

Platform	Vendor	Multi-analyte detection	Type of support surface	Type of detection	Type of biological matrix	Type of protein quantification	Sample volume requirement	Sensitivity	Dynamic range	Median intra-assay CV (%)
Proteome Profiler Antibody Arrays	R&D Systems	119	Nitrocellulose membrane	Chemiluminescence	Serum, tissue/cell lysate, urine	Semi-quantitation	–	–	–	–
Semi-quantitative antibody arrays	Abcam	96	Nitrocellulose membrane	Chemiluminescence	Serum	Semi-quantitation	0.2–1 ml	pg/ml	4-log	–
Kinex KAM microarray	Kinexus	1150	Glass slide	Fluorescence	Serum, tissue/cell lysate	Semi-quantitation	–	–	–	–
Quantitative antibody arrays	Abcam	400	Glass slide	Fluorescence	–	Absolute quantitation	50 µl	–	–	–
Full Moon direct label antibody array	Full Moon Biosystems	1358	Glass slide	Fluorescence	Serum, plasma, tissue/cell lysate	Semi-quantitation	20 µl	ng/ml	Unknown	15–50%
scioDiscover comparative protein profiling	Sciomics	1300	Glass slide	Fluorescence	Serum, plasma	Semi-quantitation	10 µl	sub ng/ml	–	<10%
Quantibody Array	Raybiotech	1000	Glass slide	Fluorescence	Serum, plasma	Absolute quantitation	1.5 ml	1–100,000 pg/ml	3- to 4-log	7–10%

–, information not available.

Performance data by the manufacturer reports high precision with an average intra-assay CV of 7 to 10% and inter-assay CV of 10 to 15%, and a dynamic range of around 3- to 4-log concentration. However, the sensitivity of the analytes varies substantially, ranging from 1 pg/ml to 100 ng/ml. A main advantage of Raybiotech is its flexibility in analyte multiplexing, offering one of the most exhaustive collections of preassembled assays, with 160 Quantibody panels available for the concurrent detection of 5 to 1000 human proteins. Kits are available for running eight samples, 22 samples, or 50 samples, with prices for the panels ranging from $197 to $4950 (for the eight sample kits). However, the sample volume requirement for the kiloplex (1000 analytes) array is 1.5 ml, meaning the micro-ELISA array may not be compatible with studies employing limited sample volumes.

Reverse-phase Protein Arrays

Reverse-phase protein arrays (RPPAs) are widely used for the quantitative, multiplexed, and high-throughput analysis of phosphorylated and total protein in tissue lysates, cultured cell lines, and biological fluids (reviewed elsewhere) (44–49). RPPA utilizes a dot-blot approach to measure the concentration of hundreds of proteins in over a thousand samples simultaneously (46, 49, 50). The samples are printed and immobilized in spots on planar microarrays (typically nitrocellulose-coated glass slides), which are subsequently incubated and probed with primary and secondary antibodies (49). Each array is printed with control samples with varying amounts of pre-determined protein concentration, to establish a calibration curve and allow for absolute protein quantification (51). Detection is achieved through colorimetric methods, fluorescence, or chemiluminescence (52). The analytical sensitivity of the technology is reported to be at the picogram to femtogram levels, with a CV of less than 10% between technical replicates (51, 52). The technology has been extensively employed for proteomics research using cell and tissue lysates, such as for tumor profiling, and demonstrated utility in therapeutic clinical research trials (47, 48, 53, 54). On the other hand, the platform is not as thoroughly explored for assessing serum matrices. The complexity and large dynamic range of the human serum matrix may pose a challenge for measuring protein levels in the picoliter of sample volume that is spotted onto the microarray (55). A few studies have demonstrated the ability of RPPA to measure up to ten serum proteins (mainly cancer biomarkers) in high-throughput formats, while assaying hundreds to thousands of samples concurrently (55–60).

Electrochemiluminescence Multiarray

Although traditional antibody arrays are time- and cost-efficient, the technique often sacrifices absolute quantification and sensitivity. A new wave of technologies has placed focus on ultrasensitivity for deep proteome profiling, reaching detection limits that are up to 1000-fold lower than traditional ELISA. The multiarray technology from Meso Scale Discovery

(MSD) is such an example, which pairs the classical sandwich-based immunoassay with ultrasensitive electro-chemiluminescence (ECL) detection to measure up to 71 proteins simultaneously in complex biological matrices. At a throughput of 960 data points in 1 to 3 min, the 123 various multiplex panels available can simultaneously measure 7 to 71 proteins, while using 10 and 25 µl of sample per well in 96- and 384-well plates, respectively. Taken together, the platform covers 180 unique human cytokines, chemokines, and bio-markers (56–62). Using the multispot technology, capture antibodies are first printed onto 96- or 384-well microtiter plates at precise, predetermined positions (Fig. 2). Subsequent incubation of the sample allows for binding of the target proteins, which are later subjected to a detection antibody that is labeled with ruthenium (II) tris-bipyridine chelate. Finally, tripropylamine (TPA) is added before the electrode surfaces of the plate are energized, causing the ruthenium label to generate an ECL signal. ECL involves an electrochemically generated intermediate that undergoes an electron transfer reaction to the electrode surface to produce excited states that emit light upon relaxation to a lower-level state (63–66). The advantages of signal transduction through ECL include high sensitivity, wide dynamic range, and stability. Often, biological samples and tissue culture media may contain molecules that are autofluorescent, which lead to high background signals when using standard fluorescence techniques (63–66). However, ECL detection lacks an excitation source and instead, relies on light emitted from bound detection antibodies that are labeled with ruthenium, thus ensuring signal specificity, high sensitivity, and minimal background (63–66). Furthermore, ECL is highly stable. When a photon is emitted through ECL, the ground state is regenerated, thus allowing for the ruthenium label to undergo many reaction cycles to release more photons (63–66). Overall, the ECL-focused immunoassays at Meso Scale provide multiplexed protein detection at a dynamic range of over 5-log with sensitivity down to sub fg/ml to sub pg/ml concentration for most analytes. Technical analysis by the manufacturer showed minimal intra-assay variability with CV of less than 20%.

Proximity Extension Assay (PEA)

Based on the principles of immuno-polymerase chain reaction (PCR), the proximity extension assay (PEA) technology runs 92-plex immunoassays in parallel to measure over 1000 proteins in 14 µl of sample (67–75). Immuno-PCR leverages the extreme sensitivity of PCR and the specificity of immunoassays to measure proteins of low abundance. The general principle of immuno-PCR consists of first allowing protein targets to bind capture antibodies and then introducing a secondary antibody that is conjugated to an oligonucleotide sequence (76–78). The formed immunocomplex is finally detected by an oligonucleotide primer that is complementary to the sequence on the secondary antibodies, to allow for DNA polymerase-dependent extension and amplification *via*

PCR (76–78). Numerous amplification cycles of the DNA amplicon product allow the signal from the immunocomplex featuring the target protein to be magnified, thereby delivering 1000 times greater sensitivity compared with traditional ELISAs (76–78). The prevalent use of immuno-PCR has mainly been tapered by complications with high background signals and long turnaround times due to the incubation and washing steps necessary in immunoassays and the amplification cycles in PCR (78). The PEA technology offered by Olink Proteomics was developed by Landegren *et al.* to use proximity-dependent DNA ligation to overcome these hurdles (79–81). The assay relies on matched pairs of antibodies that bind to adjacent epitopes on the target protein. The pairwise antibodies are conjugated to either 3′ or 5′ ends of a single-stranded DNA (ssDNA) sequence unique to the target protein, serving as a barcode. The loose ends of the strands are complementary to each other in each antibody pair (Fig. 3). Upon binding of both antibodies to the target protein, the complementary ssDNA ends on the pair of antibodies hybridize to each other as a result of their physical proximity. The hybridized structure acts as a primer that enables DNA polymerase-dependent extension in a qPCR reaction. The goal of hybridization and resulting amplification of the DNA sequence is to produce an amplified reporter DNA strand, from which the concentration of the target protein can be inferred. Signal detection is achieved through qPCR, where oligonucleotide probes labeled with distinct fluorescent tag hybridize to specific double-stranded DNA amplicons through complementary base pairing. The signal intensity of each unique amplicon is proportional to the concentration of the associated protein in the sample. In the case of the 92-plex reactions, 1 µl of a biological sample (such as serum or plasma) is channeled into a microwell and incubated with 92 pairs of matched, ssDNA-conjugated antibodies, along with DNA polymerase, detection probes, and internal controls for the hybridization, extension, and amplification steps. The dual recognition feature *via* matched, pairwise antibodies and selective hybridization of the complementary ssDNA sequences are key in reducing background signal and ensuring specificity. This effectively eliminates the wash steps in traditional immunoassays to substantially diminish the run time. However, a main disadvantage of the PEA technology is that it does not provide absolute quantification of protein concentration. Instead, the qPCR readout of the frequency of the amplicons is relayed into an arbitrary unit on a log2 scale termed, normalized protein expression (NPX), which provides a relative quantification of the associated protein present in the sample. NPX values are determined by normalizing to the median qPCR readout of a run and therefore are only comparative within the same run. For this reason, the multiplex panels using PEA are valuable tools for exploratory studies where relative protein concentrations between samples are sufficient for determining candidate targets or biomarkers. If researchers are looking for absolute quantification
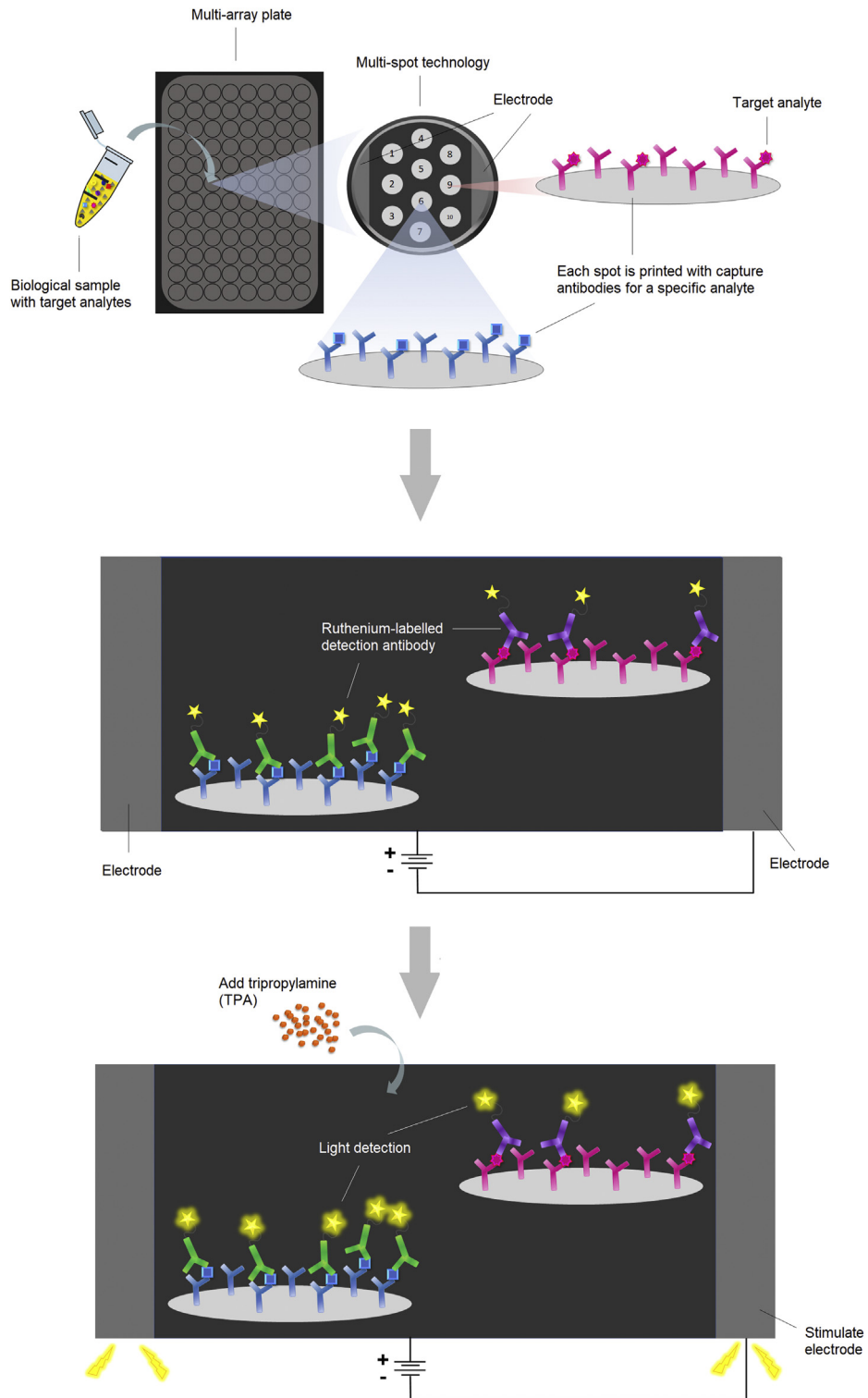
FIG. 2. **Electrochemiluminescence (ECL) multiarray.** Capture antibodies are printed onto 96- or 384-well microtiter plates at precise, predetermined positions. Each spot (1–10) is a barcode for a specific analyte of interest. Biological sample is incubated in the wells, allowing for binding of the target proteins. After washing, detection antibody that is conjugated to a ruthenium tag is added. After final wash steps, tri-propylamine (TPA) is added before the electrode surfaces of the plate are stimulated, causing the ruthenium label to create an ECL signal in the form of light. Redrawn based on https://www.mesoscale.com/en/technical_resources/our_technology.
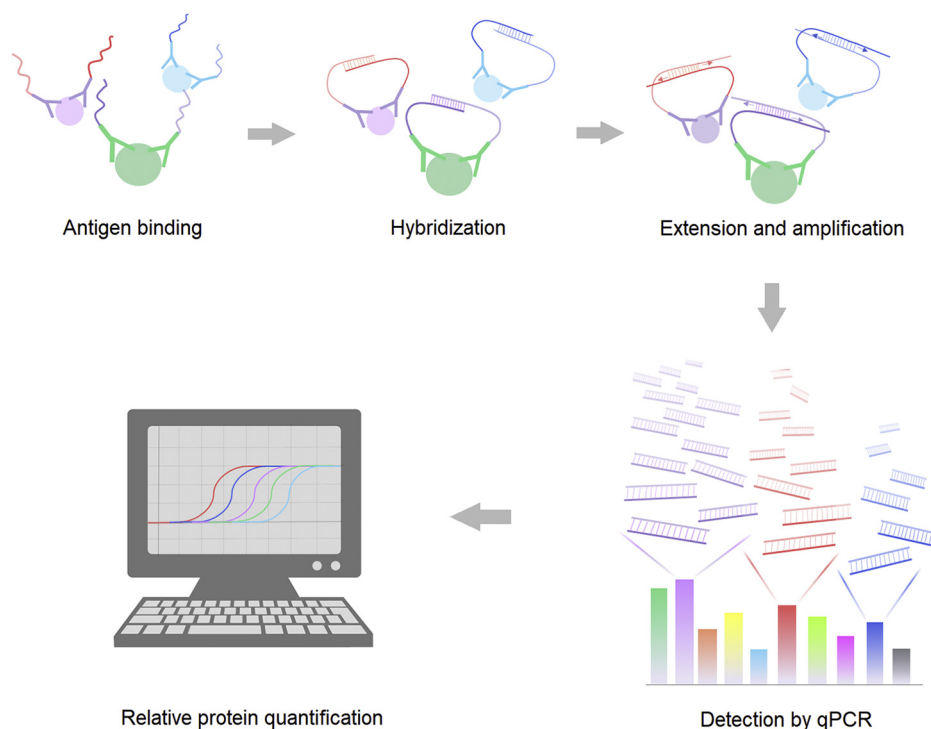
FIG. 3. **Proximity extension assay (PEA).** First, 92 pairs of antibodies that are conjugated to unique DNA sequences that are complementary to each other are incubated with the sample to allow for antigen binding. The DNA sequences on the pairwise antibodies come into proximity upon antigen binding, facilitating the complementary sequences to hybridize. DNA sequences from non-pairwise antibodies that are nonspecifically bound to the antigen are not complementary to each other and do not hybridize, thereby ensuring assay specificity. Each hybridized sequence is extended by DNA polymerase and amplified through PCR, serving as a unique DNA barcode for its corresponding target antigen. The amount of each amplified DNA sequence is detected by fluorescent readout using microfluidics qPCR. The qPCR readout of each DNA sequence, acting as a barcode to a specific target antigen, correlates to the relative concentration of the protein. Redrawn based on Toribio *et al.* (161).

of protein concentration and already have candidate biomarkers in mind, there is an option to create a custom 21-plex panel as a service provided by Olink, which would include protein calibration standards for each analyte to generate quantitative data.

PEA technology allows for concurrent analysis of 14 92-plex panels with biological relevance spanning from cardiovascular, immuno-oncology, and neurology to oncology, among others. Since the entire process is automated and 1 μl of each sample is channeled into a microwell per 92-plex reaction, 14 multiplex panels can be run in parallel using a total sample volume of 14 μl to measure 1288 proteins. Despite the merits of immunoPCR, multiplexing in qPCR is constrained by the availability of probes labeled with optically distinct fluorescent tags. To traverse this barrier, the qPCR readout detection was recently upgraded to an innovative play on next-generation sequencing (NGS) to give rise to the PEA-NGS technology, as described by Darmanis *et al.* (82). The purpose of conventional NGS techniques is to match unknown DNA sequences to a reference genome, in order to map out exomes, gene sequences, mutations, and even the whole genome. Conversely in PEA-NGS, known DNA amplicons are matched to a pre-built reference library and counted, to correlate to the

concentration of the associated target protein in the sample. This latest platform consists of running four 384-plex panels in parallel to provide 1536 protein measurements in 2.8 μl of sample. In general, 384 samples can be analyzed in a 384-well plate for each 1536-protein run, producing over 500,000 data points in less than 36 h. The new 384-plex panels yield a 6.5-fold increase in throughput compared with the 92-plex panels. Both the 92-plex and 384-plex assays span a broad dynamic range of 10-log, with sensitivity down to sub fg/ml and CVs of less than 15% for >96% of the proteins as reported by the manufacturer.

BEAD-BASED IMMUNOASSAYS
Microsphere Bead Capture

The microsphere bead capture technology by Luminex is built on the foundation of sandwich ELISA, but with the capture antibodies immobilized on 6.5-micron super-paramagnetic microsphere beads (83–85). To facilitate robust multiplexing, the beads are internally entrapped with a range of concentrations of differently colored fluorescent dyes with each optically distinct subpopulation of beads adhered to capture antibodies specific to a given analyte (Fig. 4). After the
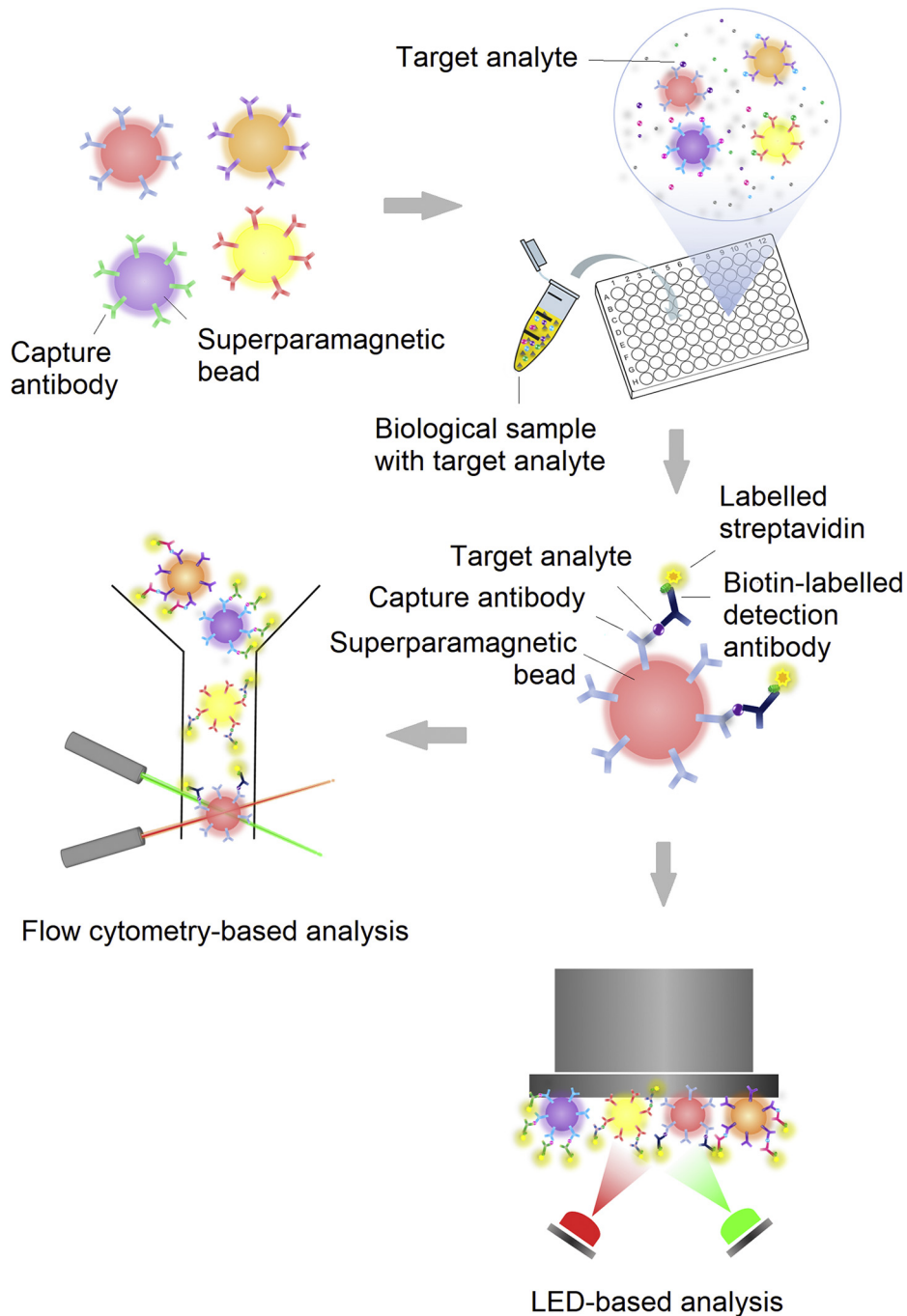
Fig. 4. **Microsphere bead capture assay.** The superparamagnetic microsphere beads are internally entrapped with a range of concentrations of differently colored fluorescent dyes with each optically distinct subpopulation of beads adhered to capture antibodies specific to a given analyte. Biological sample is incubated with the bead mixture to allow for target analyte binding. Then, secondary antibodies that are labeled with the fluorescent reporter dye, phycoerythrin (PE), are introduced and bind to the proteins. For signal detection, the content of each well is drawn into an array reader, which utilizes either a flow cytometry/laser-excitation-based system or light-emitting diode (LED)/image-based platform. A red classification laser excites the internal fluorescent dye in each bead to sort it into its specific spectral identity, corresponding to analyte specificity. A green reporter laser excites the PE conjugated to the secondary antibodies, with the PE emission intensity correlating to the concentration of the target proteins bound on each bead. The LED-based readers use microfluidics to draw the beads into a chamber, which then magnetically immobilizes the beads. Classification and reporter excitation, like in flow cytometer, are achieved by LEDs. Redrawn based on https://www.emdmillipore.com/CA/en/life-science-research/protein-detection-quantification/Immunoassay-Platform-Solutions/luminex-instruments/xmap-technology/OUGb.qB.D_kAAAFB6sYRRk_Q,nav.

binding of target proteins, secondary antibodies that are labeled with the fluorescent reporter dye, phycoerythrin (PE), are introduced and bind to the proteins. The experiment can be performed in 96- or 384-well microtiter plates, permitting for high throughput. For data acquisition, the content of each well is drawn into an array reader, which utilizes either a flow cytometry/laser-excitation-based system (Bio-Plex 100/200) or light-emitting diode (LED)/image-based platform (MAGPIX or FLEXMAP 3D). Flow cytometry was the originally developed detection method for Luminex, where precision-fluidics aligns the beads into a single file through a flow cell and each bead is subjected to a dual-excitation system. A red classification laser excites the internal fluorescent dye in each bead to sort it into its specific spectral identity, corresponding to analyte specificity. A green reporter laser excites the PE conjugated to the secondary antibodies, with the PE emission intensity correlating to the concentration of the target proteins bound on each bead. The newest LED-based readers use microfluidics to draw the beads into a chamber, which then magnetically immobilizes the beads. Classification and reporter excitation, like in flow cytometry, are achieved by LEDs. In both methods, signal recording for analyte specificity and concentration is generated at high speed with throughput of up to 1000 samples a day. The signals are converted into digital readings in real time with a detection range around 1 to 10 pg/ml and dynamic range of around 3- to 4-log (8). However, the LED-based system, FLEXMAP 3D, allows for the highest multiplexing power with up to 500 analytes being measured in 12.5 μl of sample. Currently available multiplex panels feature biologically relevant proteins, including functions in immuno-oncology, proinflammatory pathways, apoptosis pathways, kidney toxicity, immunotherapy response, immune checkpoint, cardiology, and angiogenesis, to name a few (86–92).

Single-molecule Array (Simoa)

The sensitivity of bead-based immunoassays (1–10 pg/ml) is left wanting compared with advancements in planar immunoassays (often with sensitivities at fg/ml). The single-molecule array (Simoa) technology, commercialized by Quanterix, tackled this problem with a digital bead-based sandwich ELISA that provides protein quantification down to sub fg/ml concentration (93). Paramagnetic beads are coated with the capture antibody specific to each analyte and added to a sample (Fig. 5). The beads are subsequently incubated with the biotinylated detection antibody, followed by streptavidin-B-galactosidase, to ensure that each captured target protein forms an enzyme-labeled immunocomplex. The bead mixture is then subjected to a microfluidics-integrated device, the Simoa analyzer, which involves arrays of femtoliter-sized wells that each fit exactly one bead and are filled with fluorogenic substrate. When the beads are present in large excess to the concentration of the target protein, based on Poisson distribution statistics, the

majority of beads will each bind to either none or one single target protein molecule. A negligibly small number of beads will bind more than one protein molecule. If a well contains a target protein-bound bead, the associated immunocomplex will react with the substrate and yield a fluorescent product. Due to the tremendously small reaction volume, fluorescent signal from even one immunocomplex will reach detectable threshold. As hundreds of thousands of wells are analyzed simultaneously, a digital readout of the ratio of the number of wells with and without a fluorescent signal, corresponding to the absence or presence of the target protein molecule, is efficiently generated at 68 tests per hour and 2.5 h per 96-well plate. At higher protein concentrations, each bead will carry more than one target protein and multiple corresponding enzyme labels. In this case, the average number of enzyme labels on each bead can be calculated from a measure of the average fluorescence signal intensity of the active beads. This concept allows the Simoa platform a dynamic range of 4-log of protein concentration (93). By confining the signal detection to femtoliter-sized wells, Simoa also manages to eliminate the common problem of nonspecific background signals due to the possible optical absorbance of solutions and reagents used in the assay. Owing to the minuscule volume of the detection well, only the appropriately labeled detection antibody can give off a detectable signal, making it clear-cut that each signal is associated with an immunocomplex.

Simoa technology has been developed into fully automated multiplex assays by coating distinct dye-encoded beads with specific capture antibodies and labeling them with different fluorescent dyes for optical discrimination of the subpopulations of beads (93–95). Simoa technology currently allows for the simultaneous detection of 2 to 12 proteins in human biological matrices, with biological functions categorized as chemokines, cytokines, neurological molecules, and angiogenesis factors (96–102). The 10-plex panel requires 12.5 μl of serum or plasma sample and achieved a lower limit of quantification (LLOQ; threshold where protein concentration can be confidently quantified) of 100 to 1400 fg/ml for all proteins (103). The main advantage of Simoa is ultrasensitivity and high precision with a median CV of <10% as reported by the manufacturer. Although ultrasensitivity is desirable for probing the deep proteome, the existing limitations in multiplexing hinders the use of Simoa for drug target and biomarker discovery as there can be tens to hundreds of culprits in aberrant protein pathways that contribute to pathogenesis.

Slow Off-rate Modified Aptamer

The slow off-rate modified aptamer (SOMAmers) assay (SOMAscan) from SOMAlogic uses the concept of high-affinity aptamers to reach new heights in multiplex capability for protein detection without compromising ultrasensitivity (104–106). Aptamers are short oligonucleotide sequences that
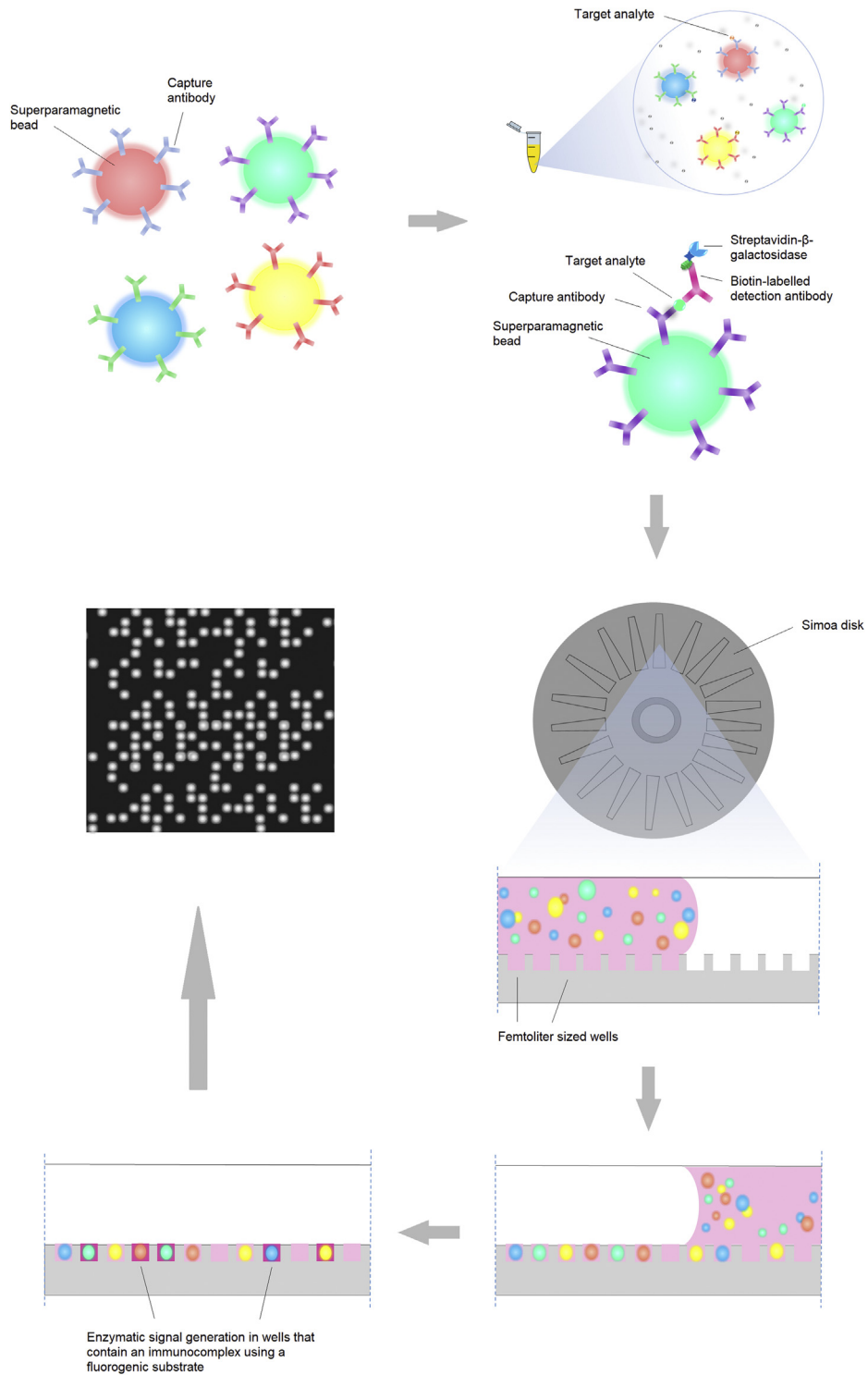
FIG. 5. **Single-molecule array (Simoa).** Paramagnetic beads are coated with the capture antibody specific to each analyte and added to a sample for target analyte binding. The beads are then incubated with the biotinylated detection antibody, followed by streptavidin-B-galactosidase, to ensure that each captured target protein forms an enzyme-labeled immunocomplex. The bead mixture is then subjected to a microfluidics-integrated device, the Simoa disk analyzer, which involves arrays of femtoliter-sized wells that each fit exactly one bead. The beads will settle into the wells and the wells are subsequently filled with fluorogenic substrate. The wells containing a bead with an immunocomplex will generate an enzymatic signal, which is detected as a fluorescent signal. Redrawn based on Cohen *et al.* and Lambert *et al.* (162, 163).

bind to a single protein target with high affinity. Aptamers are developed through many cycles of affinity selection for the oligonucleotide sequence that binds to the target protein with the highest avidity and specificity (107, 108). The nucleic acid side chains in aptamers are further modified to improve stability and affinity in biological matrices (109). These modifications, usually found at the deoxyuridine triphosphate (dUTP) regions, often imitate the hydrophobic properties of the amino acids, tryptophan, and phenylalanine, which are found naturally in various protein–protein binding sites (109). The resulting aptamers possess high affinity for the target analyte with extremely low dissociation constants of less than 1 nM and are compatible with fluorophore labeling, making them ideal for multiplexed reactions (107, 108). The workflow for SOMAscan is as follows: each SOMAmer is modified with a biotin, photocleavable group, and fluorescent tag. After incubating the SOMAmer mixture with the sample, any formed aptamer–protein complexes are captured by streptavidin-coated beads. The proteins are then labeled with biotin before the complexes are released from the beads through photocleavage and washing. Subsequently, another set of beads is added to the mixture to recapture the SOMAmer-target complexes by the biotinylated proteins. Elution using specific pH conditions releases the SOMAmers, which can then hybridize to corresponding complementary DNA sequences on a proprietary microarray chip. These long incubation and wash steps, plus the addition of polyanionic competitors, such as dextran sulfate, deter nonspecific and cross-reactive interactions with irrelevant proteins. Thus, only the SOMAmers that are unequivocally bound to their target will remain at the end of the arduous process. Lastly, the concentrations of SOMAmers, correlating to the concentrations of the target proteins, are quantified by fluorescence intensity.

In the recent years, the multiplexing ability of the SOMAscan assay evolved from measuring 1305 human proteins to quantifying up to 7000 analytes simultaneously in a volume of 55 μl serum, plasma, and other biological sample with ultrasensitivity (claimed LLOQ of 125 fg/ml) (110–117). An 8- to 10-log dynamic range is attained through three serial dilutions of every sample in efforts to detect high- and low-abundance proteins (118). In general, 85 study samples and 11 control samples are run on each 96-well plate. The workflow is highly automated to allow for efficient multiplexing and high throughput, where 680 study samples are analyzed per day. Despite the broad coverage and high throughput, the technical variability of the assay showed a median CV of 3.5% for 5000 protein measurements (119). Specifically, 50% of SOMAmers show a CV of less than 4.6%, while 95% of the SOMAmers show a CV of less than 10% (119). There are also possible caveats of the aptamer-based assay, particularly with target specificity. Joshi *et al.* (120) showed that 7% of SOMAmers showed cross-reactivity to a different protein,

27.6% detected nonhuman plasma proteins at greater signal intensity, and 35% displayed altered affinity for their target in the presence of single-nucleotide polymorphisms in individuals.

Encoded Porous Gel Microparticle

Setting itself apart from the microsphere bead capture technology, the encoded gel microparticles are made of porous bio-inert hydrogel that allows for target capture in its 3D space (121). Compared with solid magnetic beads that adhere targets on its surface, porous gel particles possess considerably higher surface-to-volume ratio for immobilizing capture antibodies (122). The porous gel FirePlex microparticles, commercialized by Abcam, support 2×10^8 higher binding capacity per particle, translating to broader dynamic range and enhanced sensitivity. The gel microparticle is cuboidal in shape with dimensions of $40 \times 40 \times 220$ microns and contains functional regions (Fig. 6). The center contains antibodies against the target protein and the two ends contain distinct fluorescent labels acting as a barcode. In the center 3D section of the particles, the target analytes bind to the capture antibodies. Then, biotin-labeled detection antibodies are added, followed by the addition of streptavidin-conjugated to a reporter dye. Finally, contents in the microwell are subjected to triple-recognition flow cytometry for data generation. The green channel excites all three sections of the particle to record its presence. The red channel excites the center region with signal from the labeled targets being proportional to analyte concentration. The yellow channel generates signals from the two end regions, where their varying fluorescence intensities act as unique barcodes for each specific analyte. An advantage of the gel microparticle is its compatibility with common flow cytometers (Millipore's Guava EasyCyte, BD Biosciences' Accuri, and Thermo Fisher's Attune). To enhance technical reliability, on average, 20 gel microparticles specific to each analyte are incubated with each sample, producing 20 reads per analyte and over 2700 data points per 96-well plate in 2.5 h. The average assay sensitivity is 500 fg/ml, with <10% CV, and a dynamic range of 4- to 5-log concentration across all analytes, which are significant improvements from the widely used microsphere bead capture-based systems. The microparticle technology that is run in 96-well plates allows for multiplexing of up to 70 proteins (mainly cytokines and inflammatory markers) in 12.5 μl of sample per well (123–125). The cost of the 70-plex assay for a 96-well plate is US$9385. More recently, the FirePlex immunoassay is made available for analysis using 384-well and 1536-well plates with a minimal sample volume requirement of 6.5 μl and 2.5 μl per well, respectively. Each 384- and 1536-well plate measures up to ten and five analytes and costs US$990 and US$1330, respectively. An automated workflow enables readouts to be generated in 20 min for the 384-well assay and in an hour for the 1536-well assay. However, this
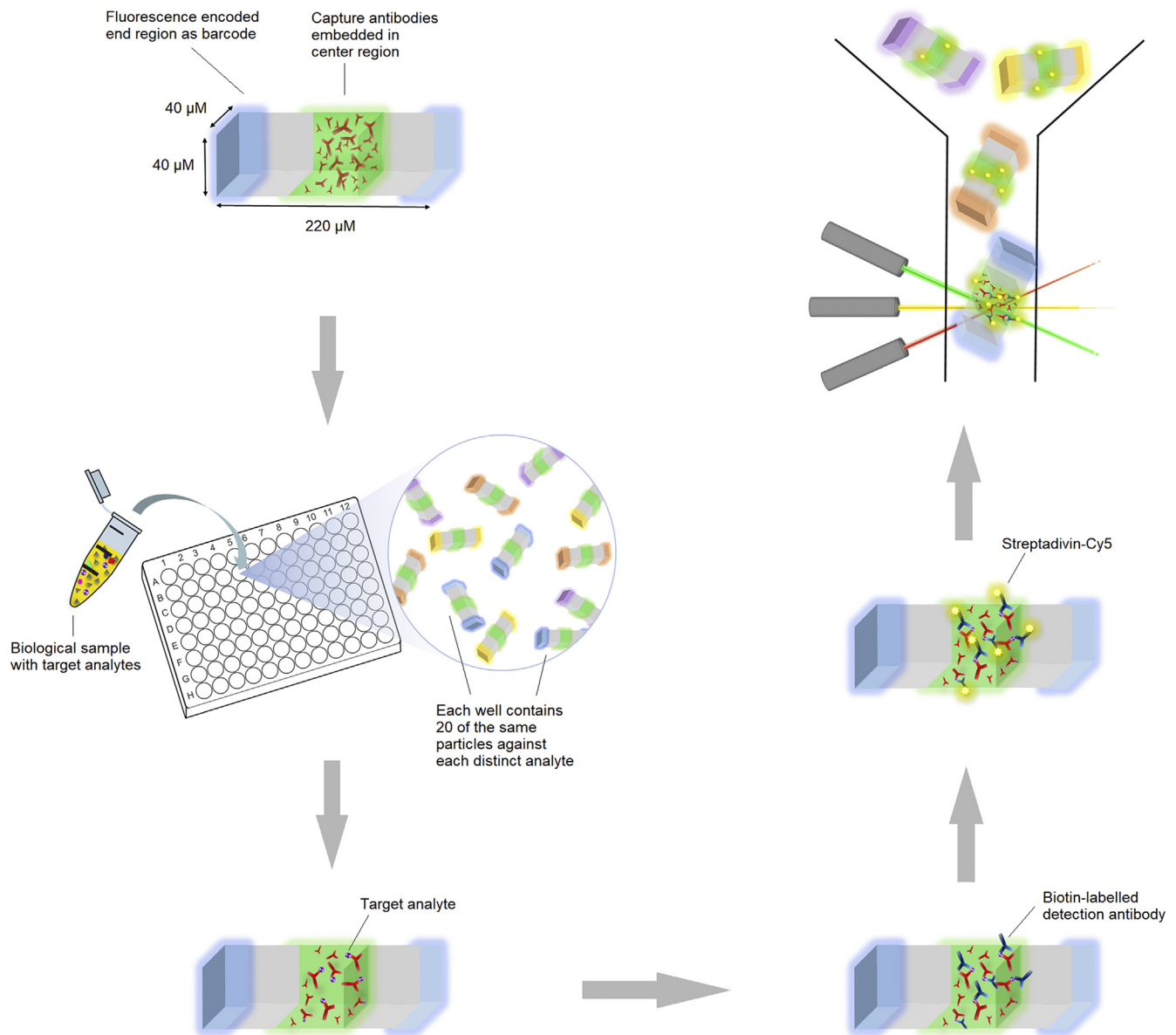
FIG. 6. **Encoded gel microparticle capture assay.** The gel microparticle is *cuboidal* in shape with dimensions of 40 × 40 × 220 microns and contains functional regions. The center contains antibodies against the target protein and the two ends contain distinct fluorescent labels acting as a barcode. Biological sample is added to the wells and incubated with the gel microparticles. Each well contains 20 of the sample micro-particles for each target protein to generate 20 signals per analyte per well. Following target binding, biotin-labeled detection antibody binding, and labeling with a streptavidin-conjugated reporter dye in the center 3D section of the particles, contents in the microwell are subjected to triple-recognition flow cytometry for data generation. The *green channel* excites all three sections of the particle to record its presence. The *red channel* excites the center region with signal from the labeled targets being proportional to analyte concentration. The *yellow channel* generates signals from the two end regions, where their varying fluorescent intensity acts as unique barcodes for each specific analyte. Redrawn based on https://www.abcam.com/kits/fireplex-particle-technology-1 and https://www.abcam.com/kits/multiplex-immunoassays-fully-customizable-and-highly-sensitive.

considerable advancement in throughput comes with hindered analytical parameters compared with the 96-well assay, where the analytical sensitivity of the 384-well and 1536-well assays ranges from 1 to 100 pg/ml, with <15% intraplate CV, and a dynamic range of 2.5 to 3 logs, according to the manufacturer (123–125).

Microsphere Bead Chip

Another twist on the microsphere bead capture technology is the novel chip-based assay from AYOXXA Biosystems, which merges the merits of antibody-coated microspheres with the exceptional throughput of planar microarrays.

Microbeads bound to capture antibodies for specific targets are fit snugly and immobilized onto the bottom surface of microwells on a chip. Each planar chip is proved unique with a random distribution of the different subpopulations of microbeads to eliminate density and location bias. A log of each chip records the precise location and capture antibody type on each microbead to spatially map out the identity of each analyte. The workflow of the microsphere bead chip assay mimics that of a sandwich ELISA, where 3 µl of sample is incubated in a chip well to allow for target binding. Fluorophore-tagged detection antibodies are added to yield immunocomplexes that are finally detected through imaging of the chip. Each chip carries thousands of microbeads bound to different antibodies, which are visualized in high resolution. The analyte concentration is calculated by the mean fluorescence intensity emitted by the hundreds of microbeads carrying the same capture antibody. This is converted into a numerical intensity value that correlates to the protein concentration. The LUNARIS Reader records the mean fluorescence intensity for each microbead and antibody pair to provide fully automated readouts of a 96-well array in approximately 10 min and a 384-well array in less than an hour. By aligning the chips into proprietary frames that can accommodate either 96 or 384 wells, the chips are compatible with equipment used for standard microtiter plates for convenience. The 96-well format allows for the analysis of 40 samples in duplicate, while the 384-well format allows for the analysis of 160 samples in duplicate. With over a hundred data points per analyte, the redundancy assures signal detection of low abundance analytes, with claimed sensitivity down to sub pg/ml, a dynamic range of 3- to 4-logs, and an intra-assay CV of <10%. Compared with conventional bead-based immunoassays that are performed in suspension, the microsphere bead chip assay mitigates some technical inconsistencies caused by the aggregation of beads, competition for binding sites, density and sedimentation artifacts, and signal quenching, where fluorescent signal intensity may be reduced in suspension formats due to proximity with neighboring fluorophore-tagged antibodies that are in excited states (126). Currently, 3 to 12 human proteins can be detected concurrently, with biological functions categorized into inflammation/cytokines, ophthalmology, and immuno-oncology (127–132).

LIMITATIONS AND TECHNICAL COMPARISONS

With fierce competition and ongoing evolutions of multiplex proteomics technologies, it is a matter of time before these platforms become commonplace for global profiling of the human proteome. We summarize the analytical features of each commercial immunoassay-based technology in Table 2. The trade-off between technical reliability and highly multiplexed protein detection comes with challenges that researchers should take into account when selecting the right proteomics tool. Nonspecific binding remains a major problem

TABLE 2

Technical parameters of commercial immunoassay-based multiplex proteomics platforms

Platform	Vendor	Multi-analyte detection	Type of biological matrix	Sample volume requirement	Sensitivity	Dynamic range	Median intra-assay CV (%)
Antibody arrays	See Table 1	Up to 1300	Serum, plasma, tissue/cell lysate	10 µl–1.5 ml	sub pg/ml–ng/ml	3- to 4-log	15–50%
Electrochemiluminescence (ECL) multiarray	Meso Scale Discovery	71	Serum, plasma, cell culture supernatants, PBMCs[a], urine	10–25 µl	sub fg/ml–pg/ml	5-log	<20%
Proximity extension assay (PEA)	Olink Proteomics	1196	Serum, plasma, tissue/cell lysate, CSF[b], urine, saliva, etc[c]	13 µl	fg/ml–pg/ml	10-log	8%
Microsphere bead capture assay	Luminex	500	Serum, plasma	13 µl	1–10 pg/ml	3- to 4-log	10%
Single-molecule array (Simoa)	Quanterix	12	Serum, plasma, tissue/cell lysate	13 µl	sub fg/ml	4-log	10%
Slow off-rate modified aptamer (SOMAmer) assay	SomaLogic	5000	Serum, plasma, tissue/cell lysate, CSF[b]	50 µl	100 fg/ml	8-log	4.6%
Encoded gel microparticle capture assay	Abcam	75	Serum, plasma	12.5 µl	500 fg/ml	4- to 5-log	<10%
Microsphere bead chip-based assay	AYOXXA	12	Serum	3 µl	sub pg/ml	3- to 4-log	<10%

[a]Peripheral blood mononuclear cell.
[b]Cerebrospinal fluid.
[c]A variety of other sample types are compatible such as fine needle biopsies, micro-dialysis fluid, dried blood spots, synovial fluid, plaque extract, and saliva.

for measuring multiple analytes, which can occur between molecules in a complex sample, with assay reagents, and the structural surface of the devices. Nonspecific binding of antibodies can hinder target binding and amplify background noise, hence reducing the signal and underrepresenting the actual protein concentration. Biological samples also often contain interfering substances that can increase the background signal. An eclectic array of proprietary assay reagents, blockers, and surface pretreatment methods have been incorporated in each platform to address this issue. The validation of high-affinity reagents, such as antibodies and aptamers, is also critical to ensure they do not cross-react with the myriad of biomolecules in an assay. Furthermore, some proteins exist in various isoforms and configurations in addition to their native form, hence necessitating a mixture of high-affinity reagents that recognize the assortment. It is crucial for all analytes to perform well to avoid false discoveries. For example, a 1% false discovery rate among 1000 analytes will yield ten false-positive hits that will require time and costs to validate separately only to fail validation.

In a race to attain the next generation of ultrasensitivity, it is critical not to overlook the dynamic range. As the concentrations of different proteins can span 12 orders of magnitude in biofluids, it is valuable to not only focus on quantifying low abundance proteins but also embodying the highly abundant ones. Some known and potential cancer biomarkers have shown to fluctuate by many orders of magnitude in healthy *versus* disease states (133–135). Many proteins that are potentially predictive of treatment response also exhibit radically altered levels in response to drug administration, whether in situations of favorable or adverse effects (136, 137). Therefore, a wide dynamic range is essential for analyzing different biological samples to compare the different levels of proteins in conditions such as healthy, benign *versus* malignant conditions, or before and after treatment.

Besides the analytical parameters of accuracy, sensitivity, and dynamic range, the reproducibility of an assay is also associated with technical superiority. Few studies have directly compared the reproducibility and concordance of results from various ultrasensitive platforms to each other. Yeung *et al.* (138) performed a cross-platform assessment of nine ultrasensitive technologies, including ECL multiarray (Meso Scale), microsphere bead capture assay (Milliplex which uses Luminex technology), Simoa, and high-sensitivity ELISA (from eBioscience or R&D Systems), for measuring four cytokines in human serum. Simoa showed an intra-assay CV of ≤10% and interassay CV of ≤14%, Meso Scale showed ≤14% and ≤26%, and Luminex exhibited ≤17% and ≤23%. In comparison, the high-sensitivity ELISA showed ≤17 to 22% intra- and inter-assay CV. Simoa showed the highest sensitivity with lower detection limits of 0.02 to 0.28 pg/ml, while Meso Scale ranged from 0.38 to 2.36 pg/ml, and Luminex ranged from 0.49 to 2.93 pg/ml. As a benchmark, the high-sensitivity ELISA yielded sensitivities ranging from 0.32 to

0.50 pg/ml. Finally, Luminex showed poor pairwise Pearson correlation with Meso Scale, Simoa, and ELISA results (r = −0.18 to 0.58) for all four cytokines. Simoa and Meso Scale showed high correlation with each other and ELISA (r ≥ 0.80) for IL-6. TNFα showed weak correlation between Simoa, Meso Scale and ELISA (r = 0.46–0.56). IL-2 and IL-17a showed poor correlation across all the comparisons. In another study, Schipke *et al.* (139) showed high correlation of measurement for three biomarkers of Alzheimer's disease in cerebrospinal fluid using the ECL multiarray from Meso Scale compared with ELISA (r = 0.80–0.99). Correlation between Meso Scale and Luminex platforms for measuring five proteins biomarkers of kidney injury in urine showed analyte-dependent correlation (r = 0.086–0.935) (140). Similarly, Chowdhury *et al.* (141) found analyte-dependent reliability for plasma cytokine profiling, where Luminex showed higher precision and Meso Scale had higher sensitivity overall. Two studies have observed favorable correlation of PEA with ELISA in candidate biomarkers for ovarian cancer and glioma (114, 142). A latest study employed the micro-ELISA array from Raybiotech to identify new diagnostic biomarkers in ovarian cancer and validated nine candidates using ELISA (143). However, Ren *et al.* (41) reported incongruities between the micro-ELISA array and ELISA data for nine protein candidates in pancreatic cancer. The overall findings illustrated that inconsistencies in protein quantification between different ultrasensitive multiplex immunoassays are highly analyte-dependent. These comparison studies highlight the importance of validating assay performance with reliable reference standards, such as the orthogonal ELISA, to avoid technical inconsistencies that can tamper biomarker discovery and drug development efforts.

An expanding selection of multiplexed proteomics tools has enabled multiplatform approaches to biomarker discovery. A multiplatform investigation revealed complementarity and correlation of PEA to untargeted LC-MS/MS in the detection and quantification of plasma proteins (144). Graumann *et al.* (114) identified ovarian cancer biomarkers using PEA and cross-validated the findings with SOMAscan, demonstrating high interplatform correlation and concordance with ELISA. A large study used SOMAscan to map 3622 plasma proteins with genetic associations and used PEA to cross-validate the expression of 266 proteins (145). The study illustrated a valuable application of novel multiplex proteomics technologies for tethering genetic factors to pathologic protein pathways to aid in the discovery of novel therapeutic targets and drug development (145). Giudice *et al.* (146) employed SOMAscan to measure >1000 plasma proteins to identify a five-marker signature of acquired aplastic anemia, which was validated with Luminex. Complementarity of SOMAscan to LC-MS/MS was also observed for enhancing the molecular characterization of mesenchymal stem cells, where both methods showed comparable reproducibility and dynamic range (147). Notably, SOMAscan elucidated very low-abundant proteins that were below the detection limit of

LC-MS/MS (147). With increasing demand for large-scale proteomics, there is a need for further investigations into the analytical inconsistencies for multianalyte detection across the various commercial multiplex technologies. Cross-validation using different multiplex platforms can also promote transparency on the technical merits of each platform and, more importantly, avoid false discovery.

FUTURE PERSPECTIVES AND CONCLUSIONS

Reviewing the advantages and disadvantages of commercial multiplex proteomics technologies brings a final word of caution. The biomedical literature has long been plagued with issues of irreproducibility, including with protein biomarker discovery using global proteomics approaches (148–152). The reasons for this are many and relate to poor study design, convenient but low-quality samples, inappropriate statistical analysis, and unreliable analytical methods. For the latter it is imperative to evaluate new multiplex proteomics technologies by including technical replicates and positive and negative controls for checking analytical sensitivity, specificity, and precision to verify the claims of the manufacturers. Otherwise, seemingly impressive technologies, if used under a black-box approach, can generate presumably promising but fallacious data (41, 153–155).

In the era of COVID-19 disease, there is keen interest in multiplex technologies that can quantify diverse viral antigens and antibodies in a multitude of specimens such as serum, nasopharyngeal swabs, and saliva, for diagnosis and prognosis. Some of the technologies discussed in this Review have already been tried to identify predictive proteomics signatures of clinical outcome and characterize the host response mechanisms (67, 73, 156–159). A number of these technologies are also adapted to provide quick results in a point-of-care setting (160). These new demands will undoubtedly trigger more innovations in the quest to develop advanced, next-generation diagnostics for various human diseases.

All in all, many tools have recently been developed to embrace new possibilities in uncovering the depths of the human proteome. There is emphasis on achieving ultrasensitivity beyond the means of conventional immunoassays, enhancing dynamic range to encompass the breadth of proteins in biofluids, and implementing automation to measure thousands of proteins in parallel with high reproducibility. Another major analytical goal of multiplexed assays is to curtail the sample quantity requirement and enhance throughput, to facilitate large-scale, statistically powered studies be it in translational, preclinical, or clinical phases. Considerations also need to be placed in the type of data rendered by commercial multiplex tools, which spans from fold-change calculations, to relative quantification on arbitrary scales, to absolute quantifications akin to benchmark ELISA methods. We are inevitably venturing into a new frontier in deep proteomics profiling, achieved by complementarity between traditional MS-based approaches and new targeted multiplex modalities. Applications of new multiplex proteomics tools are far-reaching, including delineating aberrant disease pathways, identifying and validating novel therapeutic targets, as well as discovering novel predictive biomarkers to guide diagnosis and treatment. With new opportunities in the proteomics field come great responsibilities in discerning whether a hypothesis-driven approach for investigating a handful of pathologically relevant proteins or a global hunt for hundreds to thousands of proteins in an unbiased, blinded fashion is best suited for questions at hand.

Author contributions—A. H. R., E. P. D., and V. K. conceptualization; E. P. D. and V. K. supervision; A. H. R. visualization; A. H. R., E. P. D., and V. K. writing—reviewing and editing.

Conflict of interest—The authors declare no competing interests.

Abbreviations—The abbreviations used are: CV, coefficient of variation; ECL, electrochemiluminescence; ELISA, enzyme-linked immunosorbent assay; LED, light-emitting diode; LC, liquid chromatography; MS, Mass spectrometry; MSD, meso scale discovery; NGS, next-generation sequencing; NPX, normalized protein expression; PCR, polymerase chain reaction; PE, phycoerythrin; PEA, proximity extension assay; Simoa, single-molecule array; SOMAmer, slow off-rate modified aptamer; ssDNA, single-stranded DNA; TPA, tripropylamine.

REFERENCES

1. Kavallaris, M., and Marshall, G. M. (2005) Proteomics and disease: Opportunities and challenges. *Med. J. Aust.* **182**, 575–579
2. Lippolis, R., and Angelis, M. D. (2016) Proteomics and human diseases. *J. Proteomics Bioinform.* **9**, 3
3. Hanash, S. (2003) Disease proteomics. *Nature* **422**, 226–232
4. Huang, W., Whittaker, K., Zhang, H., Wu, J., Zhu, S.-W., and Huang, R.-P. (2018) Integration of antibody array technology into drug discovery and development. *Assay Drug Dev. Technol.* **16**, 74–95
5. Burgess, R., and Huang, R.-P. (2016) Chapter four cancer stem cell biomarker discovery using antibody array technology. *Adv. Clin. Chem.* **73**, 109–125
6. Cohen, L., and Walt, D. R. (2018) Highly sensitive and multiplexed protein measurements. *Chem. Rev.* **119**, 293–321
7. Gool, A. V., Corrales, F., Čolović, M., Krstić, D., Oliver-Martos, B., Martínez-Cáceres, E., Jakasa, I., Gajski, G., Brun, V., Kyriacou, K., Burzynska-Pedziwiatr, I., Wozniak, L. A., Nierkens, S., García, C. P., Katrlik, J., *et al* (2020) Analytical techniques for multiplex analysis of protein biomarkers. *Expert Rev. Proteomics* **17**, 1–17
8. Skalnikova, H. K., Cizkova, J., Cervenka, J., and Vodicka, P. (2017) Advances in proteomic techniques for cytokine analysis: Focus on melanoma research. *Int. J. Mol. Sci.* **18**, 2697
9. Wingren, C. (2016) Antibody-based proteomics. *Adv. Exp. Med. Biol.* **926**, 163–179

10. Adhikari, S., Nice, E. C., Deutsch, E. W., Lane, L., Omenn, G. S., Pennington, S. R., Paik, Y.-K., Overall, C. M., Corrales, F. J., Cristea, I. M., Eyk, J. E. V., Uhlén, M., Lindskog, C., Chan, D. W., Bairoch, A., *et al*. (2020) A high-stringency blueprint of the human proteome. *Nat. Commun.* **11**, 5301

11. Timp, W., and Timp, G. (2020) Beyond mass spectrometry, the next step in proteomics. *Sci. Adv.* **6**, eaax8978

12. Xie, F., Liu, T., Qian, W.-J., Petyuk, V. A., and Smith, R. D. (2011) Liquid chromatography-mass spectrometry-based quantitative proteomics. *J. Biol. Chem.* **286**, 25443–25449

13. Angel, T. E., Aryal, U. K., Hengel, S. M., Baker, E. S., Kelly, R. T., Robinson, E. W., and Smith, R. D. (2012) Mass spectrometry-based proteomics: Existing capabilities and future directions. *Chem. Soc. Rev.* **41**, 3912–3928

14. Shi, T., Sun, X., Gao, Y., Fillmore, T. L., Schepmoes, A. A., Zhao, R., He, J., Moore, R. J., Kagan, J., Rodland, K. D., Liu, T., Liu, A. Y., Smith, R. D., Tang, K., Camp, D. G., *et al*. (2013) Targeted quantification of low ng/mL level proteins in human serum without immunoaffinity depletion. *J. Proteome Res.* **12**, 3353–3361

15. Reinders, J., Lewandrowski, U., Moebius, J., Wagner, Y., and Sickmann, A. (2004) Challenges in mass spectrometry-based proteomics. *Proteomics* **4**, 3686–3703

16. Robinson, R. A. S., Amin, B., and Guest, P. C. (2017) Proteomic methods in neuropsychiatric research. *Adv. Exp. Med. Biol.* **974**, 21–48

17. Landegren, U., and Hammond, M. (2021) Cancer diagnostics based on plasma protein biomarkers: Hard times but great expectations. *Mol. Oncol.* **15**, 1715–1726

18. Vidova, V., and Spacil, Z. (2017) A review on mass spectrometry-based quantitative proteomics: Targeted and data independent acquisition. *Anal. Chim. Acta* **964**, 7–23

19. Pappireddi, N., Martin, L., and Wühr, M. (2019) A review on quantitative multiplexed proteomics. *Chembiochem* **20**, 1210–1224

20. Kontostathi, G., Makridakis, M., Zoidakis, J., and Vlahou, A. (2019) Applications of multiple reaction monitoring targeted proteomics assays in human plasma. *Expert Rev. Mol. Diagn.* **19**, 499–515

21. Shi, T., Su, D., Liu, T., Tang, K., Camp, D. G., Qian, W., and Smith, R. D. (2012) Advancing the sensitivity of selected reaction monitoring-based targeted quantitative proteomics. *Proteomics* **12**, 1074–1092

22. Shah, K., and Maghsoudlou, P. (2016) Enzyme-linked immunosorbent assay (ELISA): The basics. *Br. J. Hosp. Med.* **77**, C98–C101

23. Tighe, P. J., Ryder, R. R., Todd, I., and Fairclough, L. C. (2015) ELISA in the multiplex era: Potentials and pitfalls. *Proteomics Clin. Appl.* **9**, 406–422

24. Chen, Z., Dodig-Crnković, T., Schwenk, J. M., and Tao, S. (2018) Current applications of antibody microarrays. *Clin. Proteomics* **15**, 7

25. Fan, Q., Zhou, J., Wang, Y., Xi, T., Ma, H., Wang, Z., Xiao, W., and Liu, Q. (2020) Chip-based serum proteomics approach to reveal the potential protein markers in the sub-acute stroke patients receiving the treatment of Ginkgo Diterpene Lactone Meglumine Injection. *J. Ethnopharmacol.* **260**, 112964

26. Yin, S.-J., Park, M.-W., Lee, B.-N., Yang, J.-M., Park, Y.-D., and Qian, G.-Y. (2021) Functional study of acetaldehyde dehydrogenase 1 (ALDH1) in keratinocytes: Microarray integrating bioinformatics approaches. *J. Biomol. Struct. Dyn.* **39**, 2133–2151

27. Arasu, U. T., Deen, A. J., Pasonen-Seppänen, S., Heikkinen, S., Lalowski, M., Kärnä, R., Härkönen, K., Mäkinen, P., Lázaro-Ibáñez, E., Siljander, P. R.-M., Oikari, S., Levonen, A.-L., and Rilla, K. (2020) HAS3-induced extracellular vesicles from melanoma cells stimulate IHH mediated c-Myc upregulation via the hedgehog signaling pathway in target cells. *Cell. Mol. Life Sci.* **77**, 4093–4115

28. Shin, D. H., Jo, J. Y., Kim, S. H., Choi, M., Han, C., Choi, B. K., and Kim, S. S. (2020) Midkine is a potential therapeutic target of tumorigenesis, angiogenesis, and metastasis in non-small cell lung cancer. *Cancers* **12**, 2402

29. Hannafon, B. N., Gin, A. L., Xu, Y.-F., Bruns, M., Calloway, C. L., and Ding, W.-Q. (2019) Metastasis-associated protein 1 (MTA1) is transferred by exosomes and contributes to the regulation of hypoxia and estrogen signaling in breast cancer cells. *Cell Commun. Signal.* **17**, 13

30. Luo, L., and Diamandis, E. P. (2000) Preliminary examination of time-resolved fluorometry for protein array applications. *Luminescence* **15**, 409–413

31. Yin, Y., Shelke, G. V., Lässer, C., Brismar, H., and Lötvall, J. (2020) Extracellular vesicles from mast cells induce mesenchymal transition in airway epithelial cells. *Respir. Res.* **21**, 101

32. Fultang, L., Gamble, L. D., Gneo, L., Berry, A. M., Egan, S. A., Bie, F. D., Yogev, O., Eden, G. L., Booth, S., Brownhill, S., Vardon, A., McConville, C. M., Cheng, P. N., Norris, M. D., Etchevers, H. C., *et al*. (2019) Macrophage-derived IL1β and TNFα regulate arginine metabolism in neuroblastoma. *Cancer Res.* **79**, 611–624

33. Boberg, E., Kadri, N., Winterling, J., Davies, L. C., Björklund, A., Msghina, M., Iacobaeus, E., and Blanc, K. L. (2020) Mental fatigue after allogeneic hematopoietic stem cell transplantation is associated with cognitive dysfunction, but not central nervous system inflammation. *Haematologica* **105**, e310–e314

34. Fernando, R., Wardelmann, K., Deubel, S., Kehm, R., Jung, T., Mariotti, M., Vasilaki, A., Gladyshev, V. N., Kleinridders, A., Grune, T., and Castro, J. P. (2020) Low steady-state oxidative stress inhibits adipogenesis by altering mitochondrial dynamics and decreasing cellular respiration. *Redox Biol.* **32**, 101507

35. Bakdash, G., Buschow, S. I., Gorris, M. A. J., Halilovic, A., Hato, S. V., Sköld, A. E., Schreibelt, G., Sittig, S. P., Torensma, R., Boer, T. D., Schröder, C., Smits, E. L., Figdor, C. G., and de Vries, I. J. M. (2016) Expansion of a BDCA1+CD14+ myeloid cell population in melanoma patients may attenuate the efficacy of dendritic cell vaccines. *Cancer Res.* **76**, 4332–4346

36. Reichman, H., Itan, M., Rozenberg, P., Yarmolovski, T., Brazowski, E., Varol, C., Gluck, N., Shapira, S., Arber, N., Qimron, U., Karo-Atar, D., Lee, J. J., and Munitz, A. (2019) Activated eosinophils exert anti-tumorigenic activities in colorectal cancer. *Cancer Immunol. Res.* **7**, 388–400

37. McQuilling, J. P., Burnette, M., Kimmerling, K. A., Kammer, M., and Mowry, K. C. (2019) A mechanistic evaluation of the angiogenic properties of a dehydrated amnion chorion membrane *in vitro* and *in vivo*. *Wound Repair Regen.* **27**, 609–621

38. Liang, Y., Li, J., Li, Q., Tang, L., Chen, L., Mao, Y., He, Q., Yang, X., Lei, Y., Hong, X., Zhao, Y., He, S., Guo, Y., Wang, Y., Zhang, P., *et al*. (2020) Plasma protein-based signature predicts distant metastasis and induction chemotherapy benefit in Nasopharyngeal Carcinoma. *Theranostics* **10**, 9767–9778

39. Fava, A., Buyon, J. P., Mohan, C., Zhang, T., Belmont, H. M., Izmirly, P., Clancy, R., Trujillo, J. M., Fine, D. M., Zhang, Y., Magder, L., Rao, D. A., Arazi, A., Berthier, C. C., Davidson, A., *et al*. (2020) Integrated urine proteomics and renal single-cell genomics identify an interferon-γ response gradient in lupus nephritis. *JCI Insight* **5**, e138345

40. Yang, Q., Chen, Q., Zhang, M., Cai, Y., Yang, F., Zhang, J., Deng, G., Ye, T., Deng, Q., Li, G., Zhang, H., Yi, Y., Huang, R.-P., and Chen, X. (2020) Identification of eight-protein biosignature for diagnosis of tuberculosis. *Thorax* **75**, 576–583

41. Ren, A. H., Prassas, I., Soosaipillai, A., Jarvi, S., Gallinger, S., Kulasingam, V., and Diamandis, E. P. (2020) Investigating a novel multiplex proteomics technology for detection of changes in serum protein concentrations that may correlate to tumor burden. *F1000Res.* **9**, 732

42. Palomero, J., Vegliante, M. C., Rodríguez, M. L., Eguileor, Á., Castellano, G., Planas-Rigol, E., Jares, P., Ribera-Cortada, I., Cid, M. C., Campo, E., and Amador, V. (2014) SOX11 promotes tumor angiogenesis through transcriptional regulation of PDGFA in mantle cell lymphoma. *Blood* **124**, 2235–2247

43. Schwartz, S., Wongvipat, J., Trigwell, C. B., Hancox, U., Carver, B. S., Rodrik-Outmezguine, V., Will, M., Yellen, P., de Stanchina, E., Baselga, J., Scher, H. I., Barry, S. T., Sawyers, C. L., Chandarlapaty, S., and Rosen, N. (2015) Feedback suppression of PI3Kα signaling in PTEN-mutated tumors is relieved by selective inhibition of PI3Kβ. *Cancer Cell* **27**, 109–122

44. Gallagher, R. I., and Espina, V. (2014) Reverse phase protein arrays: Mapping the path towards personalized medicine. *Mol. Diagn. Ther.* **18**, 619–630

45. Masuda, M., and Yamada, T. (2017) Signaling pathway profiling using reverse-phase protein array and its clinical applications. *Expert Rev. Proteomics* **14**, 607–615

46. Lu, Y., Ling, S., Hegde, A. M., Byers, L. A., Coombes, K., Mills, G. B., and Akbani, R. (2016) Using reverse-phase protein arrays as

pharmacodynamic assays for functional proteomics, biomarker discovery, and drug development in cancer. *Semin. Oncol.* **43**, 476–483

47. Mueller, C., Liotta, L. A., and Espina, V. (2010) Reverse phase protein microarrays advance to use in clinical trials. *Mol. Oncol.* **4**, 461–481

48. Petricoin, E., Wulfkuhle, J., Howard, M., Pierobon, M., Espina, V., Luchini, A., and Liotta, L. A. (2019) RPPA: Origins, transition to a validated clinical research tool, and next generations of the technology. *Adv. Exp. Med. Biol.* **1188**, 1–19

49. Labrie, M., Kendsersky, N. D., Ma, H., Campbell, L., Eng, J., Chin, K., and Mills, G. B. (2019) Proteomics advances for precision therapy in ovarian cancer. *Expert Rev. Proteomics* **16**, 1–10

50. Coarfa, C., Grimm, S. L., Rajapakshe, K., Perera, D., Lu, H.-Y., Wang, X., Christensen, K. R., Mo, Q., Edwards, D. P., and Huang, S. (2021) Reverse-phase protein array: Technology, application, data processing, and integration. *J. Biomol. Tech.* https://doi.org/10.7171/jbt.2021-3202-001

51. Pierobon, M., Wulfkuhle, J., Liotta, L. A., and Iii, E. F. P. (2019) Utilization of proteomic technologies for precision oncology applications. *Cancer Treat.* **178**, 171–187

52. Solís-Fernández, G., Montero-Calle, A., Alonso-Navarro, M., Fernandez-Torres, M.Á., Lledó, V. E., Garranzo-Asensio, M., Barderas, R., and Guzman-Aranguez, A. (2021) Protein microarrays for ocular diseases. *Methods Mol. Biol.* **2344**, 239–265

53. Hellström, C., Dodig-Crnković, T., Hong, M.-G., Schwenk, J. M., Nilsson, P., and Sjöberg, R. (2017) High-density serum/plasma reverse phase protein arrays. *Methods Mol. Biol.* **1619**, 229–238

54. Kuang, Z., Huang, R., Yang, Z., Lv, Z., Chen, X., Xu, F., Yi, Y.-H., Wu, J., and Huang, R.-P. (2018) Quantitative screening of serum protein biomarkers by reverse phase protein arrays. *Oncotarget* **9**, 32624–32641

55. Grote, T., Siwak, D. R., Fritsche, H. A., Joy, C., Mills, G. B., Simeone, D., Whitcomb, D. C., and Logsdon, C. D. (2008) Validation of reverse phase protein array for practical screening of potential biomarkers in serum and plasma: Accurate detection of CA19-9 levels in pancreatic cancer. *Proteomics* **8**, 3051–3060

56. [preprint] Hoepel, W., Chen, H.-J., Allahverdiyeva, S., Manz, X., Aman, J., Amsterdam UMC COVID-19 Biobank, Bonta, P., Brouwer, P., de Taeye, S., Caniels, T., van der Straten, K., Golebski, K., Griffith, G., Jonkers, R., Larsen, M., *et al.* (2020) Anti-SARS-CoV-2 IgG from severely ill COVID-19 patients promotes macrophage hyper-inflammatory responses. *bio-rxiv.* https://doi.org/10.1101/2020.07.13.190140

57. Bodnar, T. S., Raineki, C., Wertelecki, W., Yevtushok, L., Plotka, L., Zymak-Zakutnya, N., Honerkamp-Smith, G., Wells, A., Rolland, M., Woodward, T. S., Coles, C. D., Kable, J. A., Chambers, C. D., Weinberg, J., and Collaborative Initiative on Fetal Alcohol Spectrum Disorders (CIFASD). (2018) Altered maternal immune networks are associated with adverse child neurodevelopment: Impact of alcohol consumption during pregnancy. *Brain Behav. Immun.* **73**, 205–215

58. Skott, E., Yang, L. L., Stiernborg, M., Söderström, Å., Rùegg, J., Schalling, M., Forsell, Y., Giacobini, M., and Lavebratt, C. (2020) Effects of a synbiotic on symptoms, and daily functioning in attention deficit hyperactivity disorder – a double-blind randomized controlled trial. *Brain Behav. Immun.* **89**, 9–19

59. Guglielmo-Viret, V., and Thullier, P. (2007) Comparison of an electrochemiluminescence assay in plate format over a colorimetric ELISA, for the detection of ricin B chain (RCA-B). *J. Immunol. Methods* **328**, 70–78

60. Hipp, S., Tai, Y.-T., Blanset, D., Deegen, P., Wahl, J., Thomas, O., Rattel, B., Adam, P. J., Anderson, K. C., and Friedrich, M. (2017) A novel BCMA/CD3 bispecific T-cell engager for the treatment of multiple myeloma induces selective lysis *in vitro* and *in vivo*. *Leukemia* **31**, 1743–1751

61. Locke, F. L., Neelapu, S. S., Bartlett, N. L., Siddiqi, T., Chavez, J. C., Hosing, C. M., Ghobadi, A., Budde, L. E., Bot, A., Rossi, J. M., Jiang, Y., Xue, A. X., Elias, M., Aycock, J., Wiezorek, J., *et al* (2017) Phase 1 results of ZUMA-1: A multicenter study of KTE-C19 anti-CD19 CAR T cell therapy in refractory aggressive lymphoma. *Mol. Ther.* **25**, 285–295

62. Liu, K. Y. P., Lu, X. J. D., Zhu, Y. S., Le, N., Kim, H., and Poh, C. F. (2018) Plasma-derived inflammatory proteins predict oral squamous cell carcinoma. *Front. Oncol.* **8**, 585

63. Gross, E. M., Maddipati, S. S., and Snyder, S. M. (2016) A review of electrogenerated chemiluminescent biosensors for assays in biological matrices. *Bioanalysis* **8**, 2071–2089

64. Martínez-Periñán, E., Gutiérrez-Sánchez, C., García-Mendiola, T., and Lorenzo, E. (2020) Electrochemiluminescence biosensors using screen-printed electrodes. *Biosensors* **10**, 118

65. Rizwan, M., Mohd-Naim, N., and Ahmed, M. (2018) Trends and advances in electrochemiluminescence nanobiosensors. *Sensors.* **18**, 166

66. Hiramoto, K., Villani, E., Iwama, T., Komatsu, K., Inagi, S., Inoue, K. Y., Nashimoto, Y., Ino, K., and Shiku, H. (2020) Recent advances in electrochemiluminescence-based systems for mammalian cell analysis. *Micromachines (Basel)* **11**, 530

67. Valle, D. M. D., Kim-Schulze, S., Huang, H.-H., Beckmann, N. D., Nirenberg, S., Wang, B., Lavin, Y., Swartz, T. H., Madduri, D., Stock, A., Marron, T. U., Xie, H., Patel, M., Tuballes, K., Oekelen, O. V., *et al.* (2020) An inflammatory cytokine signature predicts COVID-19 severity and survival. *Nat. Med.* **26**, 1636–1643

68. Folkersen, L., Gustafsson, S., Wang, Q., Hansen, D. H., Hedman, Å. K., Schork, A., Page, K., Zhernakova, D. V., Wu, Y., Peters, J., Eriksson, N., Bergen, S. E., Boutin, T. S., Bretherick, A. D., Enroth, S., *et al.* (2020) Genomic and drug target evaluation of 90 cardiovascular proteins in 30, 931 individuals. *Nat. Metab.* **2**, 1135–1148

69. Weivoda, M. M., Chew, C. K., Monroe, D. G., Farr, J. N., Atkinson, E. J., Geske, J. R., Eckhardt, B., Thicke, B., Ruan, M., Tweed, A. J., McCready, L. K., Rizza, R. A., Matveyenko, A., Kassem, M., Andersen, T. L., *et al.* (2020) Identification of osteoclast-osteoblast coupling factors in humans reveals links between bone and energy metabolism. *Nat. Commun.* **11**, 87

70. Raeber, M. E., Rosalia, R. A., Schmid, D., Karakus, U., and Boyman, O. (2020) Interleukin-2 signals converge in a lymphoid–dendritic cell pathway that promotes anticancer immunity. *Sci. Transl. Med.* **12**, eaba5464

71. Harris, S. E., Cox, S. R., Bell, S., Marioni, R. E., Prins, B. P., Pattie, A., Corley, J., Maniega, S. M., Hernández, M. V., Morris, Z., John, S., Bronson, P. G., Tucker-Drob, E. M., Starr, J. M., Bastin, M. E., *et al.* (2020) Neurology-related protein biomarkers are associated with cognitive ability and brain volume in older age. *Nat. Commun.* **11**, 800

72. Zheng, J., Haberland, V., Baird, D., Walker, V., Haycock, P. C., Hurle, M. R., Gutteridge, A., Erola, P., Liu, Y., Luo, S., Robinson, J., Richardson, T. G., Staley, J. R., Elsworth, B., Burgess, S., *et al.* (2020) Phenome-wide Mendelian randomization mapping the influence of the plasma proteome on complex diseases. *Nat. Genet.* **52**, 1122–1131

73. Arunachalam, P. S., Wimmers, F., Mok, C. K. P., Perera, R. A. P. M., Scott, M., Hagan, T., Sigal, N., Feng, Y., Bristow, L., Tsang, O. T.-Y., Wagh, D., Coller, J., Pellegrini, K. L., Kazmin, D., Alaaeddine, G., *et al.* (2020) Systems biological assessment of immunity to mild versus severe COVID-19 infection in humans. *Science* **369**, 1210–1220

74. Carlström, K. E., Ewing, E., Granqvist, M., Gyllenberg, A., Aeinehband, S., Enoksson, S. L., Checa, A., Badam, T. V. S., Huang, J., Gomez-Cabrero, D., Gustafsson, M., Nimer, F. A., Wheelock, C. E., Kockum, I., Olsson, T., *et al.* (2019) Therapeutic efficacy of dimethyl fumarate in relapsing-remitting multiple sclerosis associates with ROS pathway in monocytes. *Nat. Commun.* **10**, 3081

75. Agasing, A. M., Wu, Q., Khatri, B., Borisow, N., Ruprecht, K., Brandt, A. U., Gawde, S., Kumar, G., Quinn, J. L., Ko, R. M., Mao-Draayer, Y., Lessard, C. J., Paul, F., and Axtell, R. C. (2020) Transcriptomics and proteomics reveal a cooperation between interferon and T-helper 17 cells in neuromyelitis optica. *Nat. Commun.* **11**, 2856

76. Adler, M., and Spengler, M. (2009) Novel strategies and tools for enhanced sensitivity in routine biomolecule analytics. *Curr. Pharm. Anal.* **5**, 390–407

77. Ryazantsev, D. Y., Voronina, D. V., and Zavriev, S. K. (2016) Immuno-PCR: Achievements and perspectives. *Biochemistry (Mosc.)* **81**, 1754–1770

78. Chang, L., Li, J., and Wang, L. (2016) Immuno-PCR: An ultrasensitive immunoassay for biomolecular detection. *Anal. Chim. Acta* **910**, 12–24

79. Fredriksson, S., Gullberg, M., Jarvius, J., Olsson, C., Pietras, K., Gústafsdóttir, S. M., Östman, A., and Landegren, U. (2002) Protein detection using proximity-dependent DNA ligation assays. *Nat. Biotechnol.* **20**, 473–477

80. Gullberg, M., Fredriksson, S., Taussig, M., Jarvius, J., Gustafsdottir, S., and Landegren, U. (2003) A sense of closeness: Protein detection by proximity ligation. *Curr. Opin. Biotechnol.* **14**, 82–86

81. Nong, R. Y., Gu, J., Darmanis, S., Kamali-Moghaddam, M., and Landegren, U. (2014) DNA-assisted protein detection technologies. *Expert Rev. Proteomics* **9**, 21–32

82. Darmanis, S., Nong, R. Y., Vänelid, J., Siegbahn, A., Ericsson, O., Fredriksson, S., Bäcklin, C., Gut, M., Heath, S., Gut, I. G., Wallentin, L., Gustafsson, M. G., Kamali-Moghaddam, M., and Landegren, U. (2011) ProteinSeq: High-performance proteomic analyses by proximity ligation and next generation sequencing. *PLoS One* **6**, e25583

83. Graham, H., Chandler, D. J., and Dunbar, S. A. (2019) The genesis and evolution of bead-based multiplexing. *Methods* **158**, 2–11

84. Vignali, D. A. A. (2000) Multiplexed particle-based flow cytometric assays. *J. Immunol. Methods* **243**, 243–255

85. Kellar, K. L., and Iannone, M. A. (2002) Multiplexed microsphere-based flow cytometric assays. *Exp. Hematol.* **30**, 1227–1237

86. Capone, F., Guerriero, E., Sorice, A., Colonna, G., Ciliberto, G., and Costantini, S. (2016) Serum cytokinome profile evaluation: A tool to define new diagnostic and prognostic markers of cancer using multiplexed bead-based immunoassays. *Mediat. Inflamm.* **2016**, 1–11

87. Koper, O. M., Kamińska, J., Kemona, H., and Dymicka-Piekarska, V. (2015) Application of the bead-based technique in neurodegeneration: A literature review. *Neurodegener. Dis.* **15**, 281–293

88. Adamcova, M., and Šimko, F. (2018) Multiplex biomarker approach to cardiovascular diseases. *Acta Pharmacol. Sin.* **39**, 1068–1072

89. O, D. F., Aalamat, Y. E., Waelkens, E., Moor, B. D., D'Hooghe, T., and Fassbender, A. (2017) Multiplex immunoassays in endometriosis an array of possibilities. *Front. Biosci.* **22**, 479–492

90. Becker, J. H., Gao, Y., Soucheray, M., Pulido, I., Kikuchi, E., Rodríguez, M. L., Gandhi, R., Lafuente-Sanchis, A., Aupí, M., Fernández-Coronado, J. A., Martín-Martorell, P., Cremades, A., Galbis-Caravajal, J. M., Alcácer, J., Christensen, C. L., *et al.* (2019) CXCR7 reactivates ERK signaling to promote resistance to EGFR kinase inhibitors in NSCLC. *Cancer Res.* **79**, 4439–4452

91. Ren, J., Cai, R., Wang, J., Daniyal, M., Baimanov, D., Liu, Y., Yin, D., Liu, Y., Miao, Q., Zhao, Y., and Chen, C. (2019) Precision nanomedicine development based on specific opsonization of human cancer patient-personalized protein coronas. *Nano Lett.* **19**, 4692–4701

92. Wang, Q., Zhang, J., Tu, H., Liang, D., Chang, D. W., Ye, Y., and Wu, X. (2019) Soluble immune checkpoint-related proteins as predictors of tumor recurrence, survival, and T cell phenotypes in clear cell renal cell carcinoma patients. *J. Immunother. Cancer* **7**, 334

93. Rissin, D. M., Fournier, D. R., Piech, T., Kan, C. W., Campbell, T. G., Song, L., Chang, L., Rivnak, A. J., Patel, P. P., Provuncher, G. K., Ferrell, E. P., Howes, S. C., Pink, B. A., Minnehan, K. A., Wilson, D. H., *et al.* (2011) Simultaneous detection of single molecules and singulated ensembles of molecules enables immunoassays with broad dynamic range. *Anal. Chem.* **83**, 2279–2285

94. Rissin, D. M., Kan, C. W., Song, L., Rivnak, A. J., Fishburn, M. W., Shao, Q., Piech, T., Ferrell, E. P., Meyer, R. E., Campbell, T. G., Fournier, D. R., and Duffy, D. C. (2013) Multiplexed single molecule immunoassays. *Lab Chip* **13**, 2902–2911

95. Gilboa, T., Maley, A. M., Ogata, A. F., Wu, C., and Walt, D. R. (2020) Sequential protein capture in multiplex single molecule arrays: A strategy for eliminating assay cross-reactivity. *Adv. Healthc. Mater.* **10**, 2001111

96. Wilson, D. H., Rissin, D. M., Kan, C. W., Fournier, D. R., Piech, T., Campbell, T. G., Meyer, R. E., Fishburn, M. W., Cabrera, C., Patel, P. P., Frew, E., Chen, Y., Chang, L., Ferrell, E. P., von Einem, V., *et al.* (2015) The Simoa HD-1 analyzer. *SLAS Technol.* **21**, 533–547

97. McCrea, M., Broglio, S. P., McAllister, T. W., Gill, J., Giza, C. C., Huber, D. L., Harezlak, J., Cameron, K. L., Houston, M. N., McGinty, G., Jackson, J. C., Guskiewicz, K., Mihalik, J., Brooks, M. A., Duma, S., *et al.* (2020) Association of blood biomarkers with acute sport-related concussion in collegiate athletes. *JAMA Netw. Open* **3**, e1919771

98. Li, D., and Mielke, M. M. (2019) An update on blood-based markers of Alzheimer's disease using the SiMoA platform. *Neurol. Ther.* **8**, 73–82

99. Rivnak, A. J., Rissin, D. M., Kan, C. W., Song, L., Fishburn, M. W., Piech, T., Campbell, T. G., DuPont, D. R., Gardel, M., Sullivan, S., Pink, B. A., Cabrera, C. G., Fournier, D. R., and Duffy, D. C. (2015) A fully-automated, six-plex single molecule immunoassay for measuring cytokines in blood. *J. Immunol. Methods* **424**, 20–27

100. Korley, F. K., Yue, J. K., Wilson, D. H., Hrusovsky, K., Diaz-Arrastia, R., Ferguson, A. R., Yuh, E. L., Mukherjee, P., Wang, K. K. W., Valadka, A. B., Puccio, A. M., Okonkwo, D. O., and Manley, G. T. (2019) Performance evaluation of a multiplex assay for simultaneous detection of four clinically relevant traumatic brain injury biomarkers. *J. Neurotrauma* **36**, 182–187

101. Zeitlberger, A. M., Thomas-Black, G., Garcia-Moreno, H., Foiani, M., Heslegrave, A. J., Zetterberg, H., and Giunti, P. (2018) Plasma markers of neurodegeneration are raised in Friedreich's ataxia. *Front. Cell Neurosci.* **12**, 366

102. Olsen, D. A., Kjaer, I. M., and Brandslund, I. (2018) Development of a three-plex single molecule immunoassay enabling measurement of the EGFR ligands amphiregulin, betacellulin and transforming growth factor α simultaneously in human serum samples. *J. Immunol. Methods* **459**, 63–69

103. Zarozinski, C. C., Johnson, J. M., Yan, Y., Beauregard, K. G., Stadler, P. B., Patel, P., Rissin, D. M., and Ball, A. J. (2019) Development of a high sensitivity 10-plex human cytokine assay using SIMOA™ planar array technology. *J. Immunol.* [abstract]

104. Brody, E., Gold, L., Mehan, M., Ostroff, R., Rohloff, J., Walker, J., and Zichi, D. (2012) Life's simple measures: Unlocking the proteome. *J. Mol. Biol.* **422**, 595–606

105. Mehan, M. R., Ostroff, R., Wilcox, S. K., Steele, F., Schneider, D., Jarvis, T. C., Baird, G. S., Gold, L., and Janjic, N. (2013) Highly multiplexed proteomic platform for biomarker discovery, diagnostics, and therapeutics. *Adv. Exp. Med. Biol.* **734a**, 283–300

106. Lollo, B., Steele, F., and Gold, L. (2014) Beyond antibodies: New affinity reagents to unlock the proteome. *Proteomics* **14**, 638–644

107. Ochsner, U. A., Green, L. S., Gold, L., and Janjic, N. (2014) Systematic selection of modified aptamer pairs for diagnostic sandwich assays. *Biotechniques* **56**, 125–133

108. Davies, D. R., Gelinas, A. D., Zhang, C., Rohloff, J. C., Carter, J. D., O'Connell, D., Waugh, S. M., Wolk, S. K., Mayfield, W. S., Burgin, A. B., Edwards, T. E., Stewart, L. J., Gold, L., Janjic, N., and Jarvis, T. C. (2012) Unique motifs and hydrophobic interactions shape the binding of modified DNA ligands to protein targets. *Proc. Natl. Acad. Sci. U. S. A.* **109**, 19971–19976

109. Ochsner, U. A., Green, L. S., Rice, T. P., Olivas, E., Janjic, N., and Katilius, E. (2019) Targeting unique epitopes on highly similar proteins GDF-11 and GDF-8 with modified DNA aptamers. *Biochemistry* **58**, 4632–4640

110. Xiong, H., Yan, J., Cai, S., He, Q., Peng, D., Liu, Z., and Liu, Y. (2019) Cancer protein biomarker discovery based on nucleic acid aptamers. *Int. J. Biol. Macromol.* **132**, 190–202

111. Sher, A. A., Gao, A., and Coombs, K. M. (2020) Autophagy modulators profoundly alter the astrocyte cellular proteome. *Cells* **9**, 805

112. Chirinos, J. A., Zhao, L., Jia, Y., Frej, C., Adamo, L., Mann, D., Shewale, S. V., Millar, J. S., Rader, D. J., French, B., Brandimarto, J., Margulies, K. B., Parks, J. S., Wang, Z., Seiffert, D. A., *et al.* (2020) Reduced apolipoprotein M and adverse outcomes across the spectrum of human heart failure. *Circulation* **141**, 1463–1476

113. Govaere, O., Cockell, S., Tiniakos, D., Queen, R., Younes, R., Vacca, M., Alexander, L., Ravaioli, F., Palmer, J., Petta, S., Boursier, J., Rosso, C., Johnson, K., Wonders, K., Day, C. P., *et al.* (2020) Transcriptomic profiling across the nonalcoholic fatty liver disease spectrum reveals gene signatures for steatohepatitis and fibrosis. *Sci. Transl. Med.* **12**, eaba4448

114. Graumann, J., Finkernagel, F., Reinartz, S., Stief, T., Brödje, D., Renz, H., Jansen, J. M., Wagner, U., Worzfeld, T., von Strandmann, E. P., and Müller, R. (2019) Multi-platform affinity proteomics identify proteins linked to metastasis and immune suppression in ovarian cancer plasma. *Front. Oncol.* **9**, 1150

115. Deterding, R. R., Wagner, B. D., Harris, J. K., and DeBoer, E. M. (2019) Pulmonary aptamer signatures in children's interstitial and diffuse lung disease. *Am. J. Respir. Crit. Care* **200**, 1496–1504

116. Shi, L., Westwood, S., Baird, A. L., Winchester, L., Dobricic, V., Kilpert, F., Hong, S., Franke, A., Hye, A., Ashton, N. J., Morgan, A. R., Bos, I., Vos, S. J. B., Buckley, N. J., ten Kate, M., *et al.* (2019) Discovery and validation of plasma proteomic biomarkers relating to brain amyloid burden by SOMAscan assay. *Alzheimers Dement.* **15**, 1478–1488

117. Fong, T. G., Chan, N. Y., Dillon, S. T., Zhou, W., Tripp, B., Ngo, L. H., Otu, H. H., Inouye, S. K., Vasunilashorn, S. M., Cooper, Z., Xie, Z.,

Marcantonio, E. R., and Libermann, T. A. (2021) Identification of plasma proteome signatures associated with surgery using SOMAscan. *Ann. Surg.* **273**, 732–742

118. Hensley, P. (2013) SOMAmers and SOMAscan – a protein biomarker discovery platform for rapid analysis of sample collections from bench top to the clinic. *J. Biomol. Tech.* **24**, S5

119. Candia, J., Cheung, F., Kotliarov, Y., Fantoni, G., Sellers, B., Griesman, T., Huang, J., Stuccio, S., Zingone, A., Ryan, B. M., Tsang, J. S., and Biancotto, A. (2017) Assessment of variability in the SOMAscan assay. *Sci. Rep.* **7**, 14248

120. Joshi, A., and Mayr, M. (2018) In aptamers they trust. *Circulation* **138**, 2482–2485

121. Appleyard, D. C., Chapin, S. C., Srinivas, R. L., and Doyle, P. S. (2011) Barcoded hydrogel microparticles for protein detection: Synthesis, assay and scanning. *Nat. Protoc.* **6**, 1761–1774

122. Chou, J., Wong, J., Christodoulides, N., Floriano, P. N., Sanchez, X., and McDevitt, J. (2012) Porous bead-based diagnostic platforms: Bridging the gaps in healthcare. *Sensors (Basel)* **12**, 15467–15499

123. Yánez, D. C., Sahni, H., Ross, S., Solanki, A., Lau, C., Papaioannou, E., Barbarulo, A., Powell, R., Lange, U. C., Adams, D. J., Barenco, M., Ono, M., D'Acquisto, F., Furmanski, A. L., and Crompton, T. (2019) IFITM proteins drive type 2 T helper cell differentiation and exacerbate allergic airway inflammation. *Eur. J. Immunol.* **49**, 66–78

124. Clos-Garcia, M., Andrés-Marin, N., Fernández-Eulate, G., Abecia, L., Lavín, J. L., van Liempd, S., Cabrera, D., Royo, F., Valero, A., Errazquin, N., Vega, M. C. G., Govillard, L., Tackett, M. R., Tejada, G., Gónzalez, E., *et al*. (2019) Gut microbiome and serum metabolome analyses identify molecular biomarkers and altered glutamate metabolism in fibromyalgia. *Ebiomedicine* **46**, 499–511

125. Lefrançais, E., Mallavia, B., Zhuo, H., Calfee, C. S., and Looney, M. R. (2018) Maladaptive role of neutrophil extracellular traps in pathogen-induced lung injury. *JCI Insight* **3**, e98178

126. Kim, S.-W., Cho, I.-H., Park, J.-N., Seo, S.-M., and Paek, S.-H. (2016) A high-performance fluorescence immunoassay based on the relaxation of quenching, exemplified by detection of cardiac troponin I. *Sensors* **16**, 669

127. Karantanos, T., Kim, H. T., Tijaro-Ovalle, N. M., Li, L., Cutler, C., Antin, J. H., Ballen, K. K., Ritz, J., Politikos, I., and Boussiotis, V. A. (2020) Assessment of a multi-cytokine profile by a novel biochip-based assay allows correlation of cytokine profiles with clinical outcomes in adult recipients of umbilical cord blood transplantation. *Bone Marrow Transplant.* **55**, 1821–1823

128. Lužnik, Z., Oellerich, S., Roesch, K., Yin, J., Zumbansen, M., Franken, L., Melles, G. R. J., and Dana, R. (2019) DMEK failure associated with innate immune activation. *Ophthalmology* **126**, 1462–1464

129. Willems, B., Tong, L., Minh, T. D. T., Pham, N. D., Nguyen, X. H., and Zumbansen, M. (2020) Novel cytokine multiplex assay for tear fluid analysis in Sjogren's syndrome. *Ocul. Immunol. Inflamm.* https://doi.org/10.1080/09273948.2020.1767792

130. Fritsch, M., Günther, S. D., Schwarzer, R., Albert, M.-C., Schorn, F., Werthenbach, J. P., Schiffmann, L. M., Stair, N., Stocks, H., Seeger, J. M., Lamkanfi, M., Krönke, M., Pasparakis, M., and Kashkar, H. (2019) Caspase-8 is the molecular switch for apoptosis, necroptosis and pyroptosis. *Nature* **575**, 683–687

131. Tijaro-Ovalle, N. M., Li, S., Defilipp, Z., Politikos, I., Joyce, R. M., Armand, P., Ho, V. T., Koreth, J., Nikiforow, S., Alyea, E. P., Avigan, D. E., Rosenblatt, J., Brown, J., McAfee, S., Dey, B., *et al* (2019) Development of HHV-6-specific immunity after cord blood transplantation in adults depends on reconstitution of thymopoiesis and regeneration of CD4+ T cells. *Blood* **134**, 3275

132. Chen, Y., Shao, C., Fan, N.-W., Nakao, T., Amouzegar, A., Chauhan, S. K., and Dana, R. (2021) The functions of IL-23 and IL-2 on driving autoimmune effector T-helper 17 cells into the memory pool in dry eye disease. *Mucosal Immunol.* **14**, 177–186

133. Forones, N. M., Tanaka, M., and Falcão, J. B. (1997) CEA as a prognostic index in colorectal cancer. *Sao Paulo Med.* **115**, 1589–1592

134. Halm, U. (2006) Perioperative CA19-9 levels can predict stage and survival in patients with resectable pancreatic adenocarcinoma. *J. Clin. Oncol.* **24**, 5610

135. Zorn, K. K., Tian, C., McGuire, W. P., Hoskins, W. J., Markman, M., Muggia, F. M., Rose, P. G., Ozols, R. F., Spriggs, D., and Armstrong, D.

K. (2009) The prognostic value of pretreatment CA 125 in patients with advanced ovarian carcinoma. *Cancer* **115**, 1028–1035

136. Pouw, J., Leijten, E., Radstake, T., and Boes, M. (2019) Emerging molecular biomarkers for predicting therapy response in psoriatic arthritis: A review of literature. *Clin. Immunol.* **211**, 108318

137. Stevens, T. W., Matheeuwsen, M., Lönnkvist, M. H., Parker, C. E., Wildenberg, M. E., Gecse, K. B., and D'Haens, G. R. (2018) Systematic review: Predictive biomarkers of therapeutic response in inflammatory bowel disease—personalised medicine in its infancy. *Aliment. Pharmacol. Ther.* **48**, 1213–1231

138. Yeung, D., Ciotti, S., Purushothama, S., Gharakhani, E., Kuesters, G., Schlain, B., Shen, C., Donaldson, D., and Mikulskis, A. (2016) Evaluation of highly sensitive immunoassay technologies for quantitative measurements of sub-pg/mL levels of cytokines in human serum. *J. Immunol. Methods* **437**, 53–63

139. Schipke, C. G., Prokop, S., Heppner, F. L., Heuser, I., and Peters, O. (2011) Comparison of immunosorbent assays for the quantification of biomarkers for Alzheimer's disease in human cerebrospinal fluid. *Dement. Geriatr. Cogn.* **31**, 139–145

140. Pavkovic, M., Riefke, B., Gutberlet, K., Raschke, M., and Ellinger-Ziegelbauer, H. (2014) Comparison of the MesoScale Discovery and Luminex multiplex platforms for measurement of urinary biomarkers in a cisplatin rat kidney injury model. *J. Pharmacol. Toxicol. Methods* **69**, 196–204

141. Chowdhury, F., Williams, A., and Johnson, P. (2009) Validation and comparison of two multiplex technologies, Luminex® and Mesoscale Discovery, for human cytokine profiling. *J. Immunol. Methods* **340**, 55–64

142. Chandran, V. I., Welinder, C., Månsson, A.-S., Offer, S., Freyhult, E., Pernemalm, M., Lund, S. M., Pedersen, S., Lehtiö, J., Marko-Varga, G., Johansson, M. C., Englund, E. M., Sundgren, P. C., and Belting, M. (2019) Ultrasensitive immunoprofiling of plasma extracellular vesicles identifies syndecan-1 as a potential tool for minimally invasive diagnosis of glioma. *Clin. Cancer Res.* **25**, 3115–3127

143. Periyasamy, A., Gopisetty, G., Subramanium, M. J., Velusamy, S., and Rajkumar, T. (2020) Identification and validation of differential plasma proteins levels in epithelial ovarian cancer. *J. Proteomics* **226**, 103893

144. [preprint] Petrera, A., von Toerne, C., Behler, J., Huth, C., Thorand, B., Hilgendorff, A., and Hauck, S. M. (2020) Multi-platforms approach for plasma proteomics: Complementarity of Olink PEA technology to mass spectrometry-based protein profiling. *biorxiv*. https://doi.org/10.1101/2020.08.04.236356

145. Sun, B. B., Maranville, J. C., Peters, J. E., Stacey, D., Staley, J. R., Blackshaw, J., Burgess, S., Jiang, T., Paige, E., Surendran, P., Oliver-Williams, C., Kamat, M. A., Prins, B. P., Wilcox, S. K., Zimmerman, E. S., *et al* (2018) Genomic atlas of the human plasma proteome. *Nature* **558**, 73–79

146. Giudice, V., Biancotto, A., Wu, Z., Cheung, F., Candia, J., Fantoni, G., Kajigaya, S., Rios, O., Townsley, D., Feng, X., and Young, N. S. (2018) Aptamer-based proteomics of serum and plasma in acquired aplastic anemia. *Exp. Hematol.* **68**, 38–50

147. Billing, A. M., Hamidane, H. B., Bhagwat, A. M., Cotton, R. J., Dib, S. S., Kumar, P., Hayat, S., Goswami, N., Suhre, K., Rafii, A., and Graumann, J. (2017) Complementarity of SOMAscan to LC-MS/MS and RNA-seq for quantitative profiling of human embryonic and mesenchymal stem cells. *J. Proteomics* **150**, 86–97

148. Fiala, C., and Diamandis, E. P. (2018) Benign and malignant scientific irreproducibility. *Clin. Biochem.* **55**, 1–2

149. Fiala, C., and Diamandis, E. P. (2017) How to reduce scientific irreproducibility: The 5-year reflection. *Clin. Chem. Lab. Med.* **55**, 1845–1848

150. Fiala, C., and Diamandis, E. P. (2017) Make researchers revisit past publications to improve reproducibility. *F1000Res.* **6**, 1717

151. Ren, A. H., Fiala, C. A., Diamandis, E. P., and Kulasingam, V. (2020) Pitfalls in cancer biomarker discovery and validation with emphasis on circulating tumor DNA. *Cancer Epidemiol. Biomarkers Prev.* **29**, 2568–2574

152. Fiala, C., and Diamandis, E. P. (2020) The outcomes of scientific debates should be published: The arivale story. *J. Appl. Lab. Med.* **5**, 1070–1075

153. Diamandis, E. P. (2004) Analysis of serum proteomic patterns for early cancer diagnosis: Drawing attention to potential problems. *J. Natl. Cancer Inst.* **96**, 353–356

154. Diamandis, E. P. (2010) Cancer biomarkers: Can we turn recent failures into success? *J. Natl. Cancer Inst.* **102**, 1462–1467

155. Prassas, I., Brinc, D., Farkona, S., Leung, F., Dimitromanolakis, A., Chrystoja, C. C., Brand, R., Kulasingam, V., Blasutig, I. M., and Diamandis, E. P. (2014) False biomarker discovery due to reactivity of a commercial ELISA for CUZD1 with cancer antigen CA125. *Clin. Chem.* **60**, 381–388

156. Consiglio, C. R., Cotugno, N., Sardh, F., Pou, C., Amodio, D., Rodriguez, L., Tan, Z., Zicari, S., Ruggiero, A., Pascucci, G. R., Santilli, V., Campbell, T., Bryceson, Y., Eriksson, D., Wang, J., *et al.* (2020) The immunology of multisystem inflammatory syndrome in children with COVID-19. *Cell* **183**, 968–981.e7

157. Pisanic, N., Randad, P. R., Kruczynski, K., Manabe, Y. C., Thomas, D. L., Pekosz, A., Klein, S. L., Betenbaugh, M. J., Clarke, W. A., Laeyendecker, O., Caturegli, P. P., Larman, H. B., Detrick, B., Fairley, J. K., Sherman, A. C., *et al.* (2020) COVID-19 serology at population scale: SARS-CoV-2-Specific antibody responses in saliva. *J. Clin. Microbiol.* **59**, e02204–e02220

158. Fraser, D. D., Cepinskas, G., Patterson, E. K., Slessarev, M., Martin, C., Daley, M., Patel, M. A., Miller, M. R., O'Gorman, D. B., Gill, S. E., Pare, G., Prassas, I., and Diamandis, E. (2020) Novel outcome biomarkers identified with targeted proteomic analyses of plasma from critically ill coronavirus disease 2019 patients. *Crit. Care Explor.* **2**, e0189

159. Pietzner, M., Wheeler, E., Carrasco-Zanini, J., Raffler, J., Kerrison, N. D., Oerton, E., Auyeung, V. P. W., Luan, J., Finan, C., Casas, J. P., Ostroff, R., Williams, S. A., Kastenmüller, G., Ralser, M., Gamazon, E. R., *et al.* (2020) Genetic architecture of host proteins involved in SARS-CoV-2 infection. *Nat. Commun.* **11**, 6397

160. Ning, B., Yu, T., Zhang, S., Huang, Z., Tian, D., Lin, Z., Niu, A., Golden, N., Hensley, K., Threeton, B., Lyon, C. J., Yin, X.-M., Roy, C. J., Saba, N. S., Rappaport, J., *et al.* (2021) A smartphone-read ultrasensitive and quantitative saliva test for COVID-19. *Sci. Adv.* **7**, eabe3703

161. Toribio, M., Fitch, K. V., Stone, L., Zanni, M. V., Lo, J., de Filippi, C., Sponseller, C. A., Lee, H., Grundberg, I., Thompson, M. A., Aberg, J. A., and Grinspoon, S. K. (2018) Assessing statin effects on cardiovascular pathways in HIV using a novel proteomics approach: Analysis of data from INTREPID, a randomized controlled trial. *Ebiomedicine* **35**, 58–66

162. Cohen, L., Hartman, M. R., Amardey-Wellington, A., and Walt, D. R. (2017) Digital direct detection of microRNAs using single molecule arrays. *Nucleic Acids Res.* **45**, gkx542

163. Lambert, J., Chang, L., Song, L., Patel, P. P., Shan, D., Johnson, J., and Rissin, D. (2018) P2-098: Comparison of two platforms quantitating fg/ml neurological biomarkers using single molecule arrays and digital ELISA: The benchtop reader SR-X[TM] and the fully automated analyzer HD-1[TM]. *Alzheimers Dement.* **14**, P706